

1 **Effects of spatially heterogeneous lakeside development on nearshore biotic communities in a large,**
2 **deep, oligotrophic lake (Lake Baikal, Siberia)**

3 Michael F. Meyer^{1*}

4 Ted Ozersky²

5 Kara H. Woo³

6 Kirill Shchapov²

7 Aaron W. E. Galloway⁴

8 Julie B. Schram⁴

9 Emma J. Rosi⁵

10 Daniel D. Snow⁶

11 Maxim A. Timofeyev⁷

12 Dmitry Yu. Karnaukhov⁷

13 Matthew R. Brousil³

14 Stephanie E. Hampton³

15 ¹. School of the Environment, Washington State University, Pullman, WA, USA

16 ². Large Lakes Observatory, University of Minnesota - Duluth, Duluth, MN, USA

17 ³. Center for Environmental Research, Education, and Outreach, Washington State University,
18 Pullman, WA, USA

19 ⁴. Oregon Institute of Marine Biology, University of Oregon, Charleston, OR, USA

20 ⁵. Cary Institute of Ecosystem Studies, Millbrook, NY, USA

21 ⁶. School of Natural Resources, University of Nebraska-Lincoln, Lincoln, NE, USA

22 ⁷. Biological Research Institute, Irkutsk State University, Irkutsk, Irkutsk Oblast, Russia

23 *corresponding author: michael.f.meyer@wsu.edu

24 **Running Head:** Baikal littoral foodwebs

25 **Keywords:** sewage, PPCP, food webs, fatty acids, human disturbance

26 **Statement of novelty, significance, and breadth of interest of the science presented in the**
27 **proposed manuscript**

28 We examined food web responses to heterogenous disturbance along the shoreline of
29 oligotrophic Lake Baikal. Using sewage-specific indicators (pharmaceuticals and personal care
30 products) we demonstrated that increased nutrients at three discrete lakeside developments (80-
31 1,963 permanent residents) and the associated increased filamentous benthic algal abundance
32 were consistent with sewage pollution. This is the first study to provide robust evidence that
33 recent benthic algal blooms are caused by sewage. These changes in benthic algae altered
34 resources and nutrition for grazing invertebrates, whose composition differed at disturbed sites.
35 Stable isotope and fatty acid analysis of benthic algae and macroinvertebrates suggested that
36 grazers at sewage disturbed sites compensate for changing resource nutrition through behavior or
37 altered metabolism. This study demonstrates how patchy, low-level eutrophication of
38 oligotrophic systems can cause food webs to respond in less visible ways.

39

40 **Statement indicating why L&O is the best outlet for the work**

41 This study will appeal to L&O readers interested in both basic and applied issues. From a basic
42 ecology perspective, we investigate how bottom-up disturbances can propagate throughout a
43 food web. From an applied perspective, we highlight how our results can inform monitoring
44 programs. Additionally, we use a suite of interdisciplinary techniques in a manner appreciated by
45 limnologists and oceanographers, such that L&O seems like the perfect home for this
46 manuscript.

47

48 **Abstract**

49 Sewage released from lakeside development can reshape ecological communities. In particular,
50 nearshore periphyton can rapidly assimilate sewage-associated nutrients, leading to increases of
51 filamentous algal abundance, thus altering both food abundance and quality for grazers. In Lake
52 Baikal, a large, ultra-oligotrophic, remote lake in Siberia, filamentous algal abundance has
53 increased near lakeside developments, and localized sewage input is the suspected cause. These
54 shifts are of particular interest in Lake Baikal, where endemic littoral biodiversity is high,
55 lakeside settlements are mostly small, tourism is relatively high (~1.2 million visitors annually),
56 and settlements are separated by large tracts of undisturbed shoreline, enabling investigation of
57 heterogeneity and gradients of disturbance. We surveyed sites along 40 km of Baikal's
58 southwestern shore for sewage indicators – pharmaceuticals and personal care products (PPCPs)
59 and microplastics – as well as periphyton and macroinvertebrate abundance and indicators of
60 food web structure (stable isotopes and fatty acids). PPCPs, including caffeine and
61 acetaminophen/paracetamol, were spatially related to lakeside development. As predicted,
62 lakeside development was associated with more filamentous algae and lower abundance of
63 sewage-sensitive mollusks. Periphyton and macroinvertebrate stable isotopes and essential fatty
64 acids suggested that food web structure otherwise remained similar across sites; yet, the
65 invariance of amphipod fatty acid composition, relative to periphyton, suggested that grazers
66 adjust behavior or metabolism to compensate for different periphyton assemblages. Our results
67 demonstrate that even low levels of human disturbance can result in spatial heterogeneity of
68 nearshore ecological responses, with potential for creating less visible effects that propagate
69 through the food web.

70

71

72 **Introduction**

73 The release of treated and untreated wastewater into aquatic ecosystems is a common human
74 disturbance that can introduce pollutants and reshape aquatic ecological communities (Moore et
75 al. 2003). Nitrogen and phosphorus are among the primary pollutants in wastewater and its
76 associated byproducts (Smith et al. 1999), yet these nutrients can also originate from disparate
77 anthropogenic and natural environmental sources, thereby complicating their use as sewage
78 indicators. For example, agriculture (Powers et al. 2016), watershed processes such as melting
79 permafrost (Turetsky et al. 2000), and changes in terrestrial plant communities (Moran et al.
80 2012) can all increase allochthonous nutrient inputs similar to sewage. Regardless of the
81 nutrients' source, biological processes can further confound sewage detection. Benthic primary
82 producers, especially those in oligotrophic systems, can assimilate nutrients quickly from the
83 water column (e.g., hours), such that elevated nutrient concentrations may not be observed
84 (Hadwen and Bunn 2005).

85

86 Because nutrients come from numerous non-sewage sources, indicators consistently associated
87 with human activity, such as enhanced $\delta^{15}\text{N}$ stable isotope signatures (Costanzo et al. 2001;
88 Camilleri and Ozersky 2019), pharmaceuticals and personal care products (PPCPs) (Rosie
89 Marshall and Royer 2012; Meyer et al. 2019) and microplastics (Barnes et al. 2009), have
90 garnered increasing attention for their usefulness as sewage indicators. Stable isotopes, such as
91 $\delta^{15}\text{N}$, have been frequently used to trace sewage pollution (Gartner et al. 2002), yet their
92 potential to indicate sewage can be obfuscated by complex terrestrial (Craine et al. 2018) and
93 aquatic (Guzzo et al. 2011) processes. PPCP studies from continental (Kolpin et al. 2002;
94 Focazio et al. 2008; Yang et al. 2018) to colloidal pore (Yang et al. 2016) scales, have shown
95 that PPCP concentrations tend to be greatest closer to their source. In addition to identifying

96 areas and periods of sewage pollution, PPCPs have also demonstrated robustness in defining
97 gradients of sewage pollution in river systems, with concentrations being directly proportional to
98 population density and inversely proportional to distance from a densely populated area (Bendz
99 et al. 2005). Similar to PPCPs, microplastics (plastic debris up to 5 mm in size) also have been
100 useful to detect sewage pollution (Li et al. 2018) along gradients of increasing human population
101 density (Klein et al. 2015), although they can sometimes originate from non-sewage sources,
102 such as shoreline debris or fishing nets (Free et al. 2014). In contrast to $\delta^{15}\text{N}$ signatures and
103 PPCPs concentrations, microplastics are typically resistant to degradation (Barnes et al. 2009),
104 providing a signal over a longer time frame than many PPCPs and nutrients in sewage. As a
105 result of each pollutant's consistent association with sewage, co-located $\delta^{15}\text{N}$, PPCP, and
106 microplastic measurements can be used to infer the spatial extent and timing of sewage pollution
107 in an ecosystem.

108

109 The effects of sewage pollution are frequently first seen in nearshore benthic communities where
110 increased nutrients alter algal species composition, abundance, nutritional quality, as well as
111 food web trophic structure. Increased filamentous algal abundance, for example, has been
112 frequently observed in areas suspected of sewage pollution (Rosenberger et al. 2008; Hampton et
113 al. 2011), likely due to benthic filamentous algae efficiently removing nutrients from the water
114 column (Hadwen and Bunn 2005; Andersson and Brunberg 2006). With a changing resource
115 base, grazing macroinvertebrate communities may likewise shift to include more detritivores or
116 species capable of consuming filamentous algae (Rosenberger et al. 2008). In addition to some
117 grazers' physical difficulty consuming filamentous algae (Mazzella and Russo 1989), there also
118 may be changes in algal nutritional quality, as filamentous algae tend to contain a different

119 mixture of essential fatty acids (EFAs) in comparison to diatoms (Kelly and Scheibling 2012),
120 which dominate periphyton communities in unimpacted ecosystems. In particular, the EFAs
121 18:3ω3 and 18:2ω6 are commonly associated with green filamentous algae (Taipale et al. 2013),
122 whereas 20:5ω3 is more associated with diatoms (Taipale et al. 2013). All EFAs are largely
123 synthesized by primary producers, and each related group produces strongly differentiated
124 multivariate signatures (Taipale et al. 2013; Galloway and Winder 2015). Consumers can acquire
125 fatty acids by grazing (Dalsgaard et al. 2003) or upgrading fatty acids at their own energetic
126 expense (Sargent and Falk-Petersen 1988; Dalsgaard et al. 2003) and often reflect the fatty acid
127 signatures of their diets. Thus, comparing consumer and producer fatty acid compositions can be
128 used to infer how grazing patterns change in response to increasing sewage pollution.

129

130 To investigate lake littoral community and food web responses to sewage pollution, we surveyed
131 40 km of Lake Baikal's shoreline for indicators of sewage pollution and metrics of benthic
132 community composition and structure. Located in Siberia, Lake Baikal is the oldest, most
133 voluminous, and deepest freshwater lake in the world (Hampton et al. 2018), with the majority of
134 Lake Baikal's biodiversity occurring in the littoral zone (Kozhova and Izmest'eva 1998). While
135 Lake Baikal's pelagic zone is generally ultra-oligotrophic (Yoshida et al. 2003; O'Donnell et al.
136 2017), nearshore areas abutting lakeside settlements have shown distinct signs of eutrophication
137 (Timoshkin et al. 2016). Much of Lake Baikal's shoreline lacks human development, and
138 Baikal's watershed is largely roadless and unpopulated (Moore et al. 2009). Despite low levels of
139 development, uncharacteristic filamentous algal blooms have been occurring throughout the lake
140 since 2010 (Kravtsova et al. 2014; Timoshkin et al. 2016; Volkova et al. 2018). While increased
141 *Ulothrix* spp. abundance historically occurs in late summer (Kozhov 1963; Kozhova and

142 Izmest'eva 1998), recent observations of *Spirogyra* spp. abundance at unprecedented levels are
143 thought to be associated with increased nearshore nutrient concentrations (Volkova et al. 2018;
144 Ozersky et al. 2018). Inadequate wastewater management in lakeside settlements is likely the
145 main driver of these nearshore algal blooms (Timoshkin et al. 2016, 2018), motivating further
146 research to identify the extent to which sewage is altering nearshore communities

147

148 Given the growing evidence that Baikal's nearshore periphyton communities are responding to
149 sewage inputs, our goal was to understand how littoral benthic community composition and
150 interactions may be changing near areas of sewage pollution. This overarching goal was divided
151 into three specific objectives:

- 152 1. identify areas of wastewater pollution using consistent sewage indicators,
153 2. assess the relationship between sewage indicators and littoral periphyton and
154 macroinvertebrate community composition, and
155 3. evaluate how food webs may restructure with increasing sewage pollution.

156 We hypothesized that (1) sewage indicators, such as PPCP concentrations, $\delta^{15}\text{N}$, and
157 microplastic densities, would increase with increasing population density and proximity of
158 lakeside development; (2) an increasing sewage signal would correlate with increased dominance
159 of filamentous benthic algae; and (3) increasing filamentous algae abundance would result in
160 changes in the abundance of different macroinvertebrate feeding guilds, reflected in community
161 composition and dietary tracers such as carbon and nitrogen stable isotopes and fatty acids.

162

163 **Methods**

164 *Site description*

165 The vast majority of Lake Baikal's 2,100-km shoreline lacks lakeside development (Moore et al.
166 2009; Timoshkin et al. 2016). Our study focused on a 40-km section of Baikal's southwestern
167 shoreline, which included three settlements of different sizes (Figure 1; Figure 2). From 19
168 through 23 August 2015, we sampled 14 littoral and 3 pelagic locations along our 40-km
169 transect. Littoral locations were chosen to capture a range of sites with varying degrees of
170 adjacent shoreline development – from “developed” (along the waterfront of human settlements)
171 to “undeveloped” (no adjacent human settlements and complete forest cover; Figure 1; Figure 2;
172 Table 1). Pelagic sites were located 2 to 5 km offshore from each of the developed sites in water
173 depths of 900 to 1300 m (Figure 1; Table 1). All littoral sites were sampled at approximately the
174 same depth (~1.25 m) at a distance of 8.90 to 20.75 m from shore (Table 1). At each site, air
175 temperature was measured with a mercury thermometer, and photographs were taken of the
176 substrate and the shoreline.

177

178 Three discrete lakeside settlements were located along our 40-km transect. The largest,
179 Listvyanka, is primarily a tourist town of approximately 2000 permanent residents, although
180 tourism can contribute significantly to the town's population with approximately 1.2 million
181 annual visitors (Interfax-Tourism 2018). The other two settlements are the villages Bolshie Koty
182 and Bolshoe Goloustnoe, which have approximately 80 and 600 permanent residents,
183 respectively. Bolshie Koty is home to two field research stations and several small tourist
184 accommodations. Bolshoe Goloustnoe has several hotels and tourist camps. Although Bolshie
185 Koty and Bolshoe Goloustnoe are built along small streams that empty into Baikal, there are no
186 upstream developed sites, meaning that any observed sewage indicators in Baikal most likely
187 originated either from Bolshie Koty or Bolshoe Goloustnoe.

188

189 *Inverse distance weighted (IDW) population calculation*

190 We recognized that sewage indicator concentrations at each sampling location may be related to
191 a sampling location's spatial position relative to both the size and proximity of neighboring
192 developed sites. Therefore, we created the inverse distance weighted (IDW) population metric to
193 compress, into a single metric, information about human population size, density, and location
194 along the shoreline as well as distance between developed sites and sampling locations. The
195 IDW metric reflects the idea that sewage pollution should be positively related to increasing
196 human density and inversely related with distance from densely populated areas (*sensu* Bendz et
197 al., 2005). Additionally, Timoshkin et al. (2018) noted that sewage enters Baikal's nearshore
198 largely through groundwater, implying that locations with more directly adjacent shoreline
199 development should experience higher sewage concentrations in the lake. Acknowledging that
200 nearshore PPCP concentrations were likely positively proportional to a developed location's
201 shoreline length, we scaled a developed site's population density by its shoreline length. This
202 scaling represents population density that directly interfaces with the lake, thereby capturing the
203 idea that sewage-associated pollutants, such as PPCPs (Karnjanapiboonwong et al. 2010) and
204 nutrients (de Vries 1972), contributed away from the shoreline can be removed via the soil
205 matrix en route to the lake.

206

207 Our calculation of IDW population was done in five steps. First, we traced polygons and
208 shorelines from satellite imagery for each developed site in Google Earth. Polygons were traced
209 for the entire area of visible development (Figure 2). Similarly, shoreline traces only reflected
210 shoreline length for which there was visible development (Figure 2). Second, polygon and line

211 geometries were downloaded from Google Earth as a .kml file. Third, the .kml file was imported
212 into the R statistical environment (R Core Team 2019) where, using the sf package (Pebesma,
213 2018), we calculated shoreline length, polygon area, and centroid location for each developed
214 site. Fourth, we joined point locations of each sampling site with the spatial polygons to calculate
215 the distance from each sampling location to each developed site's centroid. Fifth, we calculated
216 IDW population for each sampling location, using formula (1)

$$217 (1) I_j = \frac{P_{LI} * L_{LI}}{A_{LI}} + \frac{P_{BK} * L_{BK}}{A_{BK}} + \frac{P_{BGO} * L_{BGO}}{A_{BGO}}$$

218 where I is the IDW population at sampling location j , P is the population at each of the three
219 developed sites Listvyanka (LI), Bolshie Koty (BK), Bolshoe Goloustnoe (BGO), A is the area of
220 a developed site in km^2 , L is the shoreline length at a developed site in km , and D is the distance
221 from sampling site j to each developed site's centroid in km . This formulation implies that all
222 sampling locations are influenced by all three developed sites. Thus, the influence of an
223 individual developed site on each sampling location is positively influenced by the size and
224 spatial density of the population and its orientation toward the shoreline, and inversely
225 proportional to a sampling location's distance from each of the three developed sites.

226

227 *Water samples*

228 At both pelagic and littoral sites, water samples were collected for nutrient, chlorophyll,
229 microplastic, and PPCP analysis. Samples were collected by hand from 0.75 m depth for each
230 littoral site and with a bucket from aboard the Irkutsk State University "Kozhov" research vessel
231 for pelagic sites. Each water sample collection procedure is described below.

232

233 *Nutrients*

234 Water samples for nutrient analyses were collected in 150 mL glass jars that had been washed
235 with phosphate-free soap and rinsed three times with water from the sampling location. Samples
236 were collected in duplicates and immediately frozen at -20°C until processing at the A.P.
237 Vinogradov Institute of Geochemistry (Siberian Branch of the Russian Academy of Sciences,
238 Irkutsk). Samples were not filtered prior to freezing, meaning that nitrogen and ammonium
239 concentrations may potentially include intracellular nitrogen and overestimate nitrogenous forms
240 in the water column.

241
242 For each water sample, nitrate, ammonium, and total phosphorus concentrations were measured.
243 For ammonium (2016a) and nitrate (2017) concentrations, samples were analyzed with a
244 spectrophotometer following the addition of Nessler's reagent and disulfuric acid respectively.
245 Total phosphorus concentration was measured with a spectrophotometer following the addition
246 of persulfate (2016b). Concentrations are reported in mg/L.

247
248 *Chlorophyll a*
249 Water samples were collected in 1.5 L plastic bottles from a depth of approximately 0.75 m.
250 Within 12 h of collection, three subsamples (up to 150 mL each) were filtered through 25-mm
251 diameter, 0.2 µm pore size nitrocellulose filters. Filters were then placed in a 35-mm petri dish
252 and frozen in the dark until processing.

253
254 Chlorophyll samples were processed in a manner similar to that of Parsons and Strickland (1963)
255 and Lorenzen (1967). Nitrocellulose filters were ground in 90% acetone, in which chlorophyll
256 extraction was allowed to proceed overnight. Samples were then centrifuged for 15-20 minutes.

257 After centrifugation, absorbance of the chlorophyll extract was measured in a spectrophotometer
258 at 630, 645, 665, and 750 nm. Concentrations were calculated using the formula: $C =$
259 $11.64(A_{665} - A_{750}) - 2.16(A_{645} - A_{750}) - 0.1(A_{630} - A_{750}) / (V_2/V_1)$; where A is the
260 absorbance value of a particular wavelength, V₁ is the volume of the filtered water, and V₂ is the
261 volume of extract. Concentrations are reported as mg/L.

262

263 *PPCPs*

264 Water samples for PPCP analysis were collected in 250 mL amber glass bottles that were rinsed
265 with either methanol or acetone and then three times with sample water prior to collections.
266 Following collection, samples were refrigerated and kept in the dark until solid phase extraction
267 (SPE).

268

269 Within 12 h of collection, samples were filtered directly from the amber glass bottle using an in-
270 line Teflon filter holder with glass microfiber GMF (1.0 μ m pore size, WhatmanGrad 934-AH)
271 in tandem with a solid phase extraction (SPE) cartridge (200 mg HLB, Waters Corporation,
272 Milford, MA) connected to a 1-liter vacuum flask. Lab personnel wore gloves and face masks to
273 minimize contamination. Prior to filtration, SPE cartridges were primed with at least 5 mL of
274 either methanol or acetone and then washed with at least 5 mL of sample water. Rate of
275 extraction was maintained at approximately 1 drop per second. Extraction proceeded until water
276 could no longer pass through the SPE cartridge or until all collected water was filtered.

277 Cartridges were stored in Whirlpacks at -20°C until analysis for 18 PPCP residues using liquid
278 chromatography tandem mass spectrometry (LC-MS-MS) following methods of Lee et al. (2016)
279 and D'Alessio et al (2018). Concentrations are reported in μ g/L.

280

281 *Microplastics*

282 At each location, samples were collected in triplicate using 1.5 L clear plastic bottles that were
283 washed thoroughly with sample water before each collection. Samples were collected by hand
284 for each littoral site and with a metal bucket from aboard the ship for pelagic sites.

285

286 For processing, each sample was vacuum filtered on to a 47-mm diameter GF/F filter. During
287 filtration, aluminum foil was used to cover the filtration funnel to prevent contamination from
288 airborne microplastic particles. After filtration, filters were dried under vacuum pressure and
289 then stored in 50-mm petri dishes. Following filtration of all three replicates, the filtrate was
290 collected and then re-filtered through a GF/F filter as a control for contamination from the plastic
291 vacuum funnel or potentially airborne microplastics.

292

293 Microplastic counting involved visual inspection of the entire GF/F in a similar manner to
294 methods described in Hanvey et al. (2017). Visual enumeration was conducted under a stereo
295 microscope with ~100x magnification, and microplastics were classified into one of three
296 categories: fibers, fragments, or beads. For all categories, plastics were defined as observed
297 objects with apparent artificial colors, so as to not enumerate plastics potentially contributed
298 from the sampling bottle itself. Fibers were defined as smooth, long plastics with consistent
299 diameters. Fragments were defined as plastics with irregularly sharp or jagged edges. Beads were
300 defined as spherical plastics. Although we did not measure microplastic size, this technique
301 likely allowed us to reliably quantify microplastics as small as ~300 µm (Hanvey et al. 2017).
302 During enumeration, GF/Fs remained covered in the petri dish to minimize potential for

303 contamination from the air. Following enumeration of both experimental and control samples,
304 fibers, fragments, and beads enumerated in the controls were subtracted from the experimental
305 microplastic densities for each plastic type and from each replicate. One location (BK-1) had two
306 control replicates, which were averaged for each plastic type and then subtracted from the
307 experimental samples. Results are reported as the average number of microplastics/L.

308

309 *Benthic biological samples*

310 At each littoral site, periphyton and macroinvertebrates were collected for relative abundance
311 estimates and food web analysis by wading and snorkeling.

312

313 *Benthic algal collection*

314 At each littoral site, we haphazardly selected three rocks representative of local substrate. A
315 plastic stencil was used to define a surface area of each rock from which we scraped a
316 standardized 14.5 cm² patch of periphyton. Samples were preserved with Lugol's solution and
317 stored in plastic scintillation vials. Additional periphyton was collected in composite from each
318 site for fatty acid and stable isotope analysis.

319

320 Periphyton taxonomic identification and enumeration was performed by subsampling 10 µL
321 aliquots from each preserved sample. For all 10 µL aliquots, cells, filaments, and colonies were
322 counted, for the entire subsample, until at least 300 cells were identified for a given sampling
323 replicate. If the first aliquot contained less than 300 cells, we counted additional subsamples until
324 we reached at least 300 cells in total. In instances when 300 cells were counted before finishing a
325 subsample, we still counted the entire aliquot. Taxa were classified into broad categories

326 consistent with Baikal algal taxonomy (Izboldina 2007), using coarse groupings to capture
327 general patterns in relative algal abundance. As a result, algal groups consisted of diatoms,
328 *Ulothrix*, *Spirogyra*, and the green algal Order Tetrasporales.

329

330 *Benthic invertebrate collection*

331 At each littoral site, three kick-net samples were collected for assessment of benthic community
332 composition and abundance. Using a D-net, we collected macroinvertebrates by flipping over 1-3
333 rocks, and then sweeping five times in a left-to-right motion across approximately 1 m. After the
334 series of sweeps, the catch was rinsed into a plastic bucket. For each replicate, bucket contents
335 were concentrated using a 64-µm mesh and placed in glass jars with 40% ethanol (vodka; the
336 only preservative available to us at the time) for preservation and refrigerated at 4°C aboard the
337 research vessel. The 40% ethanol preservative was replaced with ~80% ethanol upon return to
338 the lab within 24 to 48 hours, and samples were stored at ~4°C.

339

340 Separate collections were conducted for invertebrate fatty acid and stable isotope analyses.
341 Invertebrates were collected using a D-net in a similar fashion as the community enumeration.
342 Additional invertebrates were also collected by hand. Collected organisms were then live-sorted,
343 identified to species, and frozen at -20°C at the field station. The samples were later transferred
344 to the lab in the US via a Dewar flask with dry ice.

345

346 Invertebrate taxonomic identification and enumeration were performed under a stereo
347 microscope. All invertebrates were identified to species with the exception of juveniles
348 (Takhteev and Didorenko (2015) for amphipods; Sitnikova (2012) for mollusks; Table 2). All

349 samples contained oligochaetes and polychaetes, but due to poor preservation, these taxa were
350 not counted. Six samples of the 42 collected were not well-preserved and were excluded from
351 further analyses, in order to reduce errors in identification. KD-1 and LI-1 were the only sites
352 with 1 sample counted. BK-2 and KD-2 each had two samples counted.

353

354 *Food web characterization*

355 To characterize littoral food webs, we analyzed carbon and nitrogen stable isotopes as well as
356 fatty acid profiles for periphyton and macroinvertebrates. Prior to isotopic and fatty acid
357 analysis, periphyton and macroinvertebrate samples were lyophilized for ~24 hours,
358 homogenized to powder, and then weighed.

359

360 *Stable isotope analysis*

361 Measurements of $\delta^{15}\text{N}$ and $\delta^{13}\text{C}$ were performed on an elemental analyzer-isotope ratio mass
362 spectrometer (EA-IRMS; Finnigan DELTAplus XP, Thermo Scientific) at the Large Lakes
363 Observatory, University of Minnesota Duluth. The EA-IRMS was calibrated against certified
364 reference materials including L-glutamic acid (NIST SRM 8574), low organic soil and sorghum
365 flour (standards B-2153 and B-2159 from Elemental Micro-analysis Ltd., Okehampton, UK) and
366 in-house standards (acetanilide and caffeine). Replicate analyses of external standards showed a
367 mean standard deviation of 0.06 ‰ and 0.09 ‰, for $\delta^{13}\text{C}$ and $\delta^{15}\text{N}$, respectively.

368

369 *Fatty acid analysis*

370 Following freeze-drying, samples were transferred to 10 mL glass centrifuge vials, and 2 mL of
371 100% chloroform was added to each under nitrogen gas. Samples remained in chloroform
372 overnight at -80°C. Fatty acid extractions generally involved three phases: (1) 100% chloroform

373 extraction, (2) chloroform-methanol extraction, and (3) fatty acid
374 extraction methods were adapted from Schram et al. (2018).

375

376 After overnight chloroform extraction, samples underwent a chloroform-methanol extraction
377 three times. To each sample, we added 1 mL cooled 100% methanol, 1 mL chloroform:methanol
378 solution (2:1), and 0.8 mL 0.9% NaCl solution. Samples were inverted three times and sonicated
379 on ice for 10 minutes. Next, samples were vortexed for 1 minute, and centrifuged for 5 minutes
380 (3,000 rpm) at 4°C. Using a double pipette technique, the lower organic layer was removed and
381 kept under nitrogen. After the third extraction, samples were evaporated under nitrogen flow, and
382 resuspended in 1.5 mL chloroform and stored at -20°C overnight.

383

384 Once resuspended in chloroform, 1 mL of chloroform extract was transferred to a glass
385 centrifuge tube with a glass syringe as well as an internal standard of 4 µL of 19-carbon fatty
386 acid. Samples were then evaporated under nitrogen, and then 1 mL of toluene and 2 mL of 1%
387 sulfuric acid-methanol was added. The vial was closed under nitrogen gas and then incubated in
388 50°C water bath for 16 hours. After incubation, samples were removed from the bath, allowed to
389 reach room temperature and stored on ice. Next, we performed a potassium carbonate-hexane
390 extraction twice. To each sample, we added 2 mL of 2% potassium bicarbonate and 5 mL of
391 100% hexane, inverting the capped vial so as to mix the solution. Samples were centrifuged for 3
392 minutes (1,500 rpm) at 4°C. The upper hexane layer was then removed and placed in a vial to
393 evaporate under nitrogen flow. Once almost evaporated, 1 mL of 100% hexane was added and
394 stored in a glass amber autosampler vial for GC/MS quantification. GC/MS quantification was
395 performed with a Shimadzu QP2020 GC/MS following Schram et al. (2018).

396

397 *Statistical analyses*

398 Total phosphorus, nitrate, ammonium, microplastic abundance and density, total PPCP
399 concentration, and $\delta^{15}\text{N}$ values in macroinvertebrate tissues were log-transformed and regressed
400 against log-transformed IDW population using a linear model. Analytically, log-transforming
401 made sites comparable, as values spanned three orders of magnitude. Physically, we assumed
402 that sewage indicators were likely subject to exponential processes (e.g., mixing, diffusion), and
403 log-transforming the data should linearize the relationships between predictor and response
404 variables. Residuals were assessed for normality and homogeneity of variance.

405

406 To assess if benthic community composition was associated with increasing sewage indicators,
407 periphyton and macroinvertebrate abundance data were each analyzed with a consistent
408 multivariate workflow. First, replicates were averaged, and taxonomic groups representing less
409 than 1% of the inter-site community were removed from analysis, in order to reduce the
410 influence of rare species on results. Second, community compositions for both periphyton and
411 macroinvertebrates were visualized using non-metric multidimensional scaling (NMDS) with a
412 Bray-Curtis similarity metric. Periphyton community compositions were calculated as relative
413 proportions, whereas invertebrate abundances were grouped at the genus-level and then square-
414 root transformed to minimize influence of more abundant taxa. Visual inspection of the NMDS
415 plot suggested that sites generally tended to separate by increasing PPCP concentrations and
416 IDW population (see Table 2). To test whether sites' benthic communities significantly differed
417 with increasing PPCP concentration and IDW population, we first used k-medoids, also known
418 as Partitioning Around the Medoids (PAM; Kaufman and Rousseeuw 2005), clustering to

419 identify an optimal number of groupings (Figure S1). For this process, we iterated through
420 multiple numbers of clusters (i.e., 1 to 10) and calculated the within-group-sum-of-squares (wss)
421 and average silhouette width. We identified the optimal number of groups when wss decreased
422 most markedly and when silhouette width was greatest (i.e., the elbow method) (Johnson and
423 Wichern 2007). To confirm the optimal number as determined by non-hierarchical PAM
424 clustering, we also used Weighted Pair-Group Centroid Clustering (WPGMC) as a hierarchical
425 approach (Sneath and Sokal 1973), which corrects for clusters that may not be strongly
426 discriminated regardless of how many samples are assigned to a given cluster (Legendre and
427 Legendre 2012). We then performed two permutational multivariate analyses of variance
428 (PERMANOVA; Anderson 2001) with 999 permutations: the first where community
429 compositions were responses to the groups identified through clustering and the second where
430 community compositions were responses to the continuous IDW population. Unlike traditional
431 multivariate analyses of variance (MANOVA), PERMANOVA does not require assumptions of
432 multivariate normality (Anderson 2001). When significant differences were identified, post-hoc
433 SIMPER analysis (Clarke 1993) was performed following the PERMANOVA to identify which
434 taxonomic groups contributed to 85% of the cumulative variance that most influenced site
435 separation.

436

437 To assess whether benthic food webs restructured with increasing sewage indicator
438 concentrations, fatty acid data were analyzed in a manner similar to periphyton and
439 macroinvertebrate abundance data. First, species' fatty acid profiles were visualized by
440 performing NMDS with Bray-Curtis similarity for all organisms' relative fatty acid abundance
441 (Figure S2). This technique broadly demonstrated that, as expected, interspecific variation in

442 fatty acid composition was greater than intraspecific variation. The same pattern was observed
443 for all fatty acids quantified as well as solely essential fatty acids (EFAs; Figure S2). Together,
444 these NMDS plots suggested that periphyton fatty acids at sites differentiated based on sewage
445 indicator concentrations, which was likely a reflection of differences in periphyton community
446 composition (Taipale et al. 2013). Among all taxa and sites, 18:3 ω 3, 18:1 ω 9, and 20:5 ω 3 had the
447 highest coefficients of variation, enabling comparisons between sites. These fatty acids tend to
448 be associated with filamentous green algae (i.e., 18:3 ω 3 and 18:1 ω 9) and diatoms (i.e., 20:5 ω 3).
449 To increase the robustness of our analysis, we expanded our approach to include major fatty
450 acids within each taxonomic group, including 18:2 ω 6 (abundant in green algae); 16:1 ω 7 and
451 14:0 (abundant in diatoms); and 16:0 (abundant in both green algae and diatoms) (Taipale et al.
452 2013). To evaluate how relative fatty acid abundance may relate to sewage pollution, we
453 assessed patterns among these seven fatty acids with both multivariate and univariate
454 approaches. Within a multivariate framework, we created two NMDS plots with Bray-Curtis
455 similarity, one just with primary producer (Figure S5) and the other with macroinvertebrate
456 (Figure S6) fatty acid profiles. Because multivariate patterns suggested fatty acid profiles may
457 relate to sewage pollution, we regressed a filamentous:diatom fatty acid ratio (Equation 2)

$$458 (2) \frac{18:3\omega 3\% + 18:1\omega 9\% + 18:2\omega 6\% + 16:0\%}{20:5\omega 3\% + 16:1\omega 7\% + 16:0\% + 14:0\%}$$

459 against log-transformed PPCP concentrations using a linear model. Additionally, we evaluated
460 how three essential fatty acids (18:3 ω 3, 18:2 ω 6, and 20:5 ω 3), lipids thought to accumulate in
461 biological systems, may differ in abundance across the sewage gradient. Therefore, we similarly
462 regressed the ratio of $\frac{18:3\omega 3\% + 18:2\omega 6\%}{20:5\omega 3\%}$ against log-transformed PPCP concentrations using a
463 linear model.

464

465 All analyses were conducted in the R statistical environment (R Core Team 2019), using the
466 tidyverse (Wickham et al. 2019), factoextra (Kassambara and Mundt 2019), cluster (Maechler et
467 al. 2019), pvclust (Suzuki et al. 2019), ggrepel (Slowikowski 2019), viridis (Garnier 2018), fs
468 (Hester and Wickham 2019), spdplyr (Sumner 2019), janitor (Firke 2020), sf (Pebesma 2018),
469 ggpubr (Kassambara 2019), ggtext (Wilke 2020), OpenStreetMap (Fellows and Stotz 2019),
470 cowplot (Wilke 2019), and vegan (Oksanen et al. 2019) packages. All data, including .kml files
471 used to calculate IDW metric, are publicly available from the Environmental Data Initiative
472 repository (Meyer et al. 2020), and all R scripts are available from the GitHub repository of this
473 project's Open Science Framework account (Meyer et al. 2015).

474

475 **Results**

476 *Water samples*

477 Nearshore water nitrate ($R^2 = 0.01$, $p = 0.68$), ammonium ($R^2 = 0.17$, $p = 0.11$), total phosphorus
478 ($R^2 = 0.14$, $p = 0.14$), and chlorophyll a ($R^2 = 0.11$, $p = 0.20$) concentrations were not
479 significantly correlated with IDW population (Figure 3). Total PPCP ($R^2 = 0.26$, $p = 0.04$)
480 concentrations were significantly related with IDW population (Figure 3). In the littoral zone,
481 PPCPs detected included caffeine, 1,7-dimethylxanthine/paraxanthine (main human metabolite
482 of caffeine), cotinine (main human metabolite of nicotine), and acetaminophen/paracetamol
483 (Table 3). Other PPCPs, including carbamazepine, diphenhydramine, thiabendazole,
484 amphetamine, methamphetamine, MDA, MDMA, morphine, phenazone, sulfachloropyridazine,
485 sulfamethazine, sulfadimethoxine, sulfamethazole, trimethoprim, and cimetidine, were not
486 detected.

487

488 Microplastics were detected in samples from both littoral and pelagic sites. Bead microplastics
489 were only detected near Listvyanka. Fibers (mean = 0.85 microplastics/L, std dev = 1.21
490 microplastics/L) and fragments (mean = 0.83 microplastics/L, std dev = 1.35 microplastics/L)
491 were the most abundant types of microplastics across all sites, whereas beads were relatively rare
492 (mean = 0.08 microplastics/L, std dev = 0.31 microplastics/L). Total microplastic densities were
493 not significantly correlated with IDW population ($R^2 = 0.01$, $p = 0.65$; Figure 3), although more
494 types of microplastics were generally observed near areas with higher IDW population values,
495 such as Listvyanka.

496

497 *Benthic biological samples*

498 *Periphyton*

499 Major taxonomic groupings of periphyton consisted of diatoms, *Tetrasporales* spp., *Spirogyra*
500 spp., and *Ulothrix* spp. K-mediods (Figures S1a; S2a) and WPGMC (Figure S3a) cluster
501 analyses of periphyton abundance demonstrated two groupings capture most variance, and visual
502 inspection of relative periphyton community abundance NMDS suggested groupings were
503 related to IDW population values (Figure 4). PERMANOVA results demonstrated that
504 periphyton communities were significantly different based on IDW population groupings ($R^2 =$
505 0.52, $p = 0.001$) and the continuous IDW population ($R^2 = 0.43$, $p = 0.001$). Post-hoc SIMPER
506 results suggested that these differences were primarily associated with sites that had higher
507 *Ulothrix* spp. and *Spirogyra* spp. relative abundance. Additionally, sites with high IDW
508 populations had lower diatom relative abundance in comparison to sites with low and moderate
509 IDW populations.

510

511 *Macroinvertebrates*
512 Taxonomic groupings included five amphipod genera: *Eulimnogammarus*, *Poekilogammarus*,
513 *Cryptoroporus*, *Brandtia* and *Pallasea*; six mollusk families: Planorbidae, Valvatidae, Baicaliidae,
514 Benedictidae, Acroloxidae, and Maackia; flatworms; caddisflies; and leeches (summarized in
515 Table S1). K-mediod cluster analysis of macroinvertebrate community composition suggested 2
516 or 3 major groupings would capture most variance (Figure S1b; S2b), whereas WPGMC
517 analyses suggested 2 groupings would enable all sites except for one to be assigned a cluster
518 (S3b). Because both forms of hierarchical and non-hierarchical clustering suggested two
519 groupings as optimal, we proceeded using two groupings. Visual inspection of NMDS suggested
520 clusters were related to IDW population (Figure 5). PERMANOVA results supported the
521 hypothesis that macroinvertebrate communities significantly differed both among our IDW
522 population groupings ($R^2 = 0.19$, $p = 0.02$) and along our continuous gradient of increasing IDW
523 population ($R^2 = 0.19$, $p = 0.02$). Post-hoc SIMPER analyses suggested that *Poekilogammarus*,
524 *Eulimnogammarus*, Valvatidae, Caddisflies, *Brandtia*, Baicaliidae, Planorbidae, *Cryptoroporus*,
525 and flatworms contributed the greatest differences between high and moderate/low IDW
526 population groupings (see Table 2).

527
528 *Food web characterization: stable isotopes and fatty acids*
529 Among periphyton and amphipod samples, $\delta^{13}\text{C}$ values ranged from -19.5 to -9.5 ‰ (Figure 6).
530 Among periphyton samples, $\delta^{15}\text{N}$ values ranged from 0.77 to 3.76 ‰, whereas amphipod $\delta^{15}\text{N}$
531 values ranged from 6.42 to 7.92 ‰.

532

533 For grazers, $\delta^{15}\text{N}$ significantly increased with IDW population ($p = 0.01$; Figure 3, Figure 6).

534 Periphyton $\delta^{15}\text{N}$ signatures did not significantly increase with IDW population ($p = 0.27$). In
535 contrast, $\delta^{13}\text{C}$ concentrations were not related with IDW population for either periphyton or
536 macroinvertebrates.

537

538 With respect to fatty acids, macroinvertebrates tended to be characterized by mono-unsaturated
539 fatty acids (MUFAs) and long-chain (i.e. ≥ 20 -Carbons) polyunsaturated fatty acids (LCPUFAs),
540 whereas periphyton tended to be characterized by short-chain (i.e., 16- and 18-Carbons)
541 polyunsaturated fatty acids (SCPUFAs) (Table 3). When comparing proportions within taxa
542 across the sewage gradient, periphyton SCPUFA proportion tended to increase (Figure S4) and
543 periphyton SAFA proportions generally decreased. In contrast, benthic macroinvertebrate fatty
544 acid class proportions tended to remain consistent across the entire gradient (Figure S4).

545

546 For both periphyton and grazers, our analyses focused mainly on the fatty acids consistently
547 associated with filamentous green algae (i.e., 18:3 ω 3, 18:1 ω 9, 18:2 ω 6, and 16:0) as well as
548 diatoms (i.e., 20:5 ω 3, 16:1 ω 7, 14:0, and 16:0). For periphyton, the ratio of green
549 filamentous:diatom-associated fatty acids significantly increased with an increasing PPCP
550 concentration ($R^2 = 0.62$; $p = 0.04$, Figure 7; S5) but not with an increasing IDW population ($p =$
551 0.08). Amphipod fatty acid ratios were not significantly related with either increasing IDW
552 population or increasing PPCP concentrations (Figure 7; S6). When focusing solely on the
553 essential fatty acids 18:3 ω 3, 18:2 ω 6, and 20:5 ω 3, the same pattern was observed in both
554 periphyton ($R^2 = 0.73$; $p = 0.02$) and amphipods (Figure 7).

555

556 **Discussion**

557 Our combined results corroborate previous findings (e.g., Timoshkin et al., 2016; 2018) that
558 sewage pollution is entering Lake Baikal's nearshore area and likely is responsible for changes in
559 nearshore benthic communities. Unlike previous studies, we were able to incorporate highly
560 specific indicators of sewage pollution and food web structure to offer direct, quantitative
561 relationships between human development and ecological responses.

562

563 *Relating human settlements to sewage indicator concentrations*

564 In agreement with our expectations, some sewage pollution indicators in the nearshore of Lake
565 Baikal were associated with size of and distance from human settlements. Total PPCP,
566 macroinvertebrate $\delta^{15}\text{N}$, and, to some degree, total phosphorus concentrations increased with
567 IDW population. These sewage gradients created by highly localized settlements are noteworthy
568 considering that Baikal's shoreline, including our study area, is largely free of lakeside
569 development (Moore et al. 2009). Furthermore, the use of sewage-associated indicators, such as
570 PPCPs and $\delta^{15}\text{N}$, proved necessary for defining sewage gradients. The use of nutrients as
571 indicators alone would not reveal sewage pollution gradients, since nutrients were not strongly
572 correlated with IDW population and could come from diverse sources. For example, melting
573 permafrost in Lake Baikal's watershed (Anisimov and Reneva 2006) and the Selenga River basin
574 (Tornqvist et al. 2014) as well as climate-driven changes in mixing processes (Swann et al. 2020)
575 have the potential to contribute substantial nutrient loadings to the nearshore. While nutrients
576 also could be contributed by agriculture (Powers et al. 2016), atmospheric deposition (Galloway
577 et al. 2004; Monteith et al. 2007; Stoddard et al. 2016), and changing terrestrial plant
578 communities (Moran et al. 2012), these are not currently known to be major sources of elevated

579 nutrients in the Baikal watershed, relative to sewage (Timoshkin et al., 2016, Timoshkin et al.,
580 2018) and permafrost melt (Anisimov & Reneva, 2006).

581

582 This is the first known study to detect PPCPs in Lake Baikal, a voluminous lake in a largely
583 unpopulated watershed. We detected PPCPs nearshore but not at our three offshore sites,
584 suggesting that sewage inputs in Baikal become diluted as pollutants move out of the nearshore
585 area. More generally, these results are important for lake monitoring, as PPCPs are robust
586 indicators of sewage pollution. Beyond Lake Baikal, these data are important for understanding
587 PPCPs' prevalence in lakes, as lakes have remained less represented in the PPCP literature in
588 comparison to lotic and subsurface systems (Meyer et al. 2019). This literature imbalance creates
589 opportunities to assess how PPCPs, and sewage pollution more broadly, may lead to differing
590 ecological responses in lotic and lentic systems. As lakes tend to have longer hydraulic residence
591 times relative to rivers and streams, pollutants may be more prone to accumulate (Yang et al.
592 2018; Meyer et al. 2019). In the case of our data, comparing contemporaneous littoral and
593 pelagic PPCP concentrations revealed littoral-pelagic sewage gradients, as PPCPs were
594 degraded, metabolized or accumulated by biota, preserved within sediments, or diluted to
595 undetectable concentrations. In the context of the entire lake, analyses of sediments have shown
596 how PPCPs can remain within lake systems for decades, thereby enabling researchers to
597 reconstruct histories of wastewater pollution in a system (Czekalski et al. 2015; Yang et al.
598 2018).

599

600 Investigating PPCP concentrations across limnic environments could also establish how
601 ecological communities respond differently not only to sewage but also to the PPCPs themselves.

602 While we focus on PPCPs as indicators of sewage, previous studies have shown that PPCPs,
603 even at concentrations we observed in Lake Baikal, can elicit biological responses from
604 physiological (e.g., del Rey et al. 2011; Feijão et al. 2020) and behavioral (e.g., Brodin et al.
605 2013; Dziewczynski et al. 2016) levels to food webs (e.g., Lagesson et al. 2016; Richmond et
606 al. 2018) and ecosystems (e.g., Rosi-Marshall et al. 2013; Richmond et al. 2019; Robson et al.
607 2020). Although our study was not designed to evaluate the ecotoxicological effects of PPCPs
608 themselves, future studies could potentially address effects of PPCPs on nearshore Baikal biota
609 by using *in situ* sewage gradients as a guide.

610

611 In contrast to PPCP concentrations and $\delta^{15}\text{N}$ values, microplastics were not associated with IDW
612 population and may be poor proxies for sewage pollution in Lake Baikal. Additionally,
613 microplastics may originate from non-sewage sources, such as agriculture (Steinmetz et al. 2016)
614 and fish nets (Eerkes-Medrano et al. 2015). Because of their long degradation time (Brandon et
615 al. 2016), microplastics can indicate accumulated pollution, which likely enables wider
616 distribution from nearshore inputs to the offshore (Fischer et al. 2016; Hendrickson et al. 2018).
617 Unlike microplastic concentrations identified in Lake Hovsgol (Free et al. 2014), Lake Superior
618 (Hendrickson et al. 2018), or Lake Erie (Eriksen et al. 2013), microplastic concentrations in
619 Baikal, as quantified by our methods, may be poor proxies for capturing pollution from
620 seasonally varying human populations. It is worth noting that since the time of our field
621 sampling, evidence has accumulated that our methods likely dramatically underestimated
622 microplastic abundance (Wang and Wang 2018; Brandon et al. 2020), and there is potential for
623 the microplastics themselves to cause deleterious ecological responses. While we focus here on
624 microplastics as an indicator of sewage pollution, microplastics are increasingly shown to disrupt

625 food web dynamics by altering grazing patterns (Green 2016) and providing carbon substrate for
626 microbial growth (Romera-Castillo et al. 2018). Recent investigations of microplastics in Lake
627 Baikal near Bolshie Koty (BK) used analogous methods and measured similarly low
628 concentrations (Karnaukhov et al. 2020). When considering Lake Baikal's large volume,
629 Karnaukov et al. (2020) noted that the number of plastic pieces may well exceed those observed
630 in other lakes, such as Lake Hovsgol. Together these growing uncertainties suggest that
631 microplastic pollution in Baikal and elsewhere deserves increased attention.

632

633 *Relating sewage indicators with benthic algal communities*

634 Congruent with our hypotheses, increasing sewage indicators tended to be associated with higher
635 relative abundance of filamentous taxa in periphyton. Previous studies investigating Baikal's
636 periphyton composition noted that areas adjacent to human development often had increased
637 abundance of filamentous algae such as *Ulothrix* and *Spirogyra* (Timoshkin et al. 2016, 2018).
638 Lake Baikal's southwestern shore historically experiences short *Ulothrix* blooms in late August
639 (Kozhov 1963), potentially confounding sewage signals with an annually occurring
640 phenomenon. Our data are consistent with the results of Timoshkin et al. (2016) and show that
641 relative abundance of filamentous algae is greatest near areas of higher lakeside development.

642

643 While community composition shifted with increasing sewage indicator concentrations,
644 periphyton $\delta^{15}\text{N}$ values did not differ along our transect. Previous studies in marine (Gartner et
645 al. 2002; Savage and Elmgren 2004; Risk et al. 2009) and freshwater (Wayland and Hobson
646 2001; Camilleri and Ozersky 2019) systems have highlighted how sewage-associated $\delta^{15}\text{N}$ can
647 increase in algal samples and even throughout the food web. Like PPCPs in our study, $\delta^{15}\text{N}$

648 values are often most enriched near the source of sewage pollution and can decrease over several
649 kilometers (Savage and Elmgren 2004), with concentrations varying based on species-specific
650 uptake rates and advective, dispersive, and diffusive transport (Gartner et al. 2002). While
651 previous studies using $\delta^{15}\text{N}$ signatures in macroalgae and vascular macrophytes have
652 successfully tracked sewage gradients (Cole et al. 2004), periphyton $\delta^{15}\text{N}$ as a sewage indicator
653 potentially can be confounded by terrestrial $\delta^{15}\text{N}$ contributions such as through agricultural
654 runoff (Chang et al. 2012). In our study, periphyton $\delta^{15}\text{N}$ signatures may be explained by
655 periphyton's typically high cell turnover rates (e.g., days; Swamikannu and Hoagland 1989)
656 dampening isotopic patterns, $\delta^{15}\text{N}$ -accumulating algal taxa being grazed more readily by
657 macroinvertebrates (Rosenberger et al. 2008), or co-limitation dynamics between ammonium and
658 nitrate (York et al. 2007; Piñón-Gimate et al. 2009).

659

660 Fatty acid analyses suggested that changes in periphyton community composition altered the
661 nutritional quality of periphyton across the pollution gradient. Periphyton fatty acid profiles from
662 sites with higher sewage pollution had higher levels of 18:3 ω 3, 18:1 ω 9, 18:2 ω 6, and 16:0
663 relative to 20:5 ω 3, 16:1 ω 7, 16:0, and 14:0 fatty acids. This pattern likely reflects the higher
664 abundance of green algae relative to diatoms (Iverson et al. 2004; Osipova et al. 2009; Taipale et
665 al. 2013; Galloway and Winder 2015; Shishlyannikov et al. 2018), which we observed from our
666 periphyton community composition analysis (Figure 3). Together, our periphyton composition
667 and fatty acid results suggest that Baikal's nearshore periphyton communities near human
668 lakeside developments are more dominated by filamentous green algae, and therefore, have
669 lower nutritional content.

670

671 Among the array of fatty acids synthesized in algal communities, essential fatty acids (EFAs) are
672 most likely to be taxonomically associated with, and influenced by, changing community
673 composition. EFAs are a subgroup of polyunsaturated fatty acids (PUFAs) that are prone to
674 accumulating in organisms (see Kelly & Scheibling, 2012). Among the eight common EFAs
675 (Taipale et al. 2013), 18:3 ω 3, 18:2 ω 6, and 20:5 ω 3 had the highest coefficients of variation
676 between sites. Because these three EFAs demonstrated the greatest variation between sites, our
677 analyses focused on how their relative abundances related to PPCP concentrations and IDW
678 populations. The fatty acids 18:3 ω 3 and 18:2 ω 6 have been previously associated with
679 filamentous algae, such as Baikalian *Ulothrix* (Osipova et al. 2009), whereas 20:5 ω 3 have
680 previously been associated with Baikalian diatoms (Shishlyannikov et al. 2018). Comparing the
681 ratio of filamentous green algae to diatoms could therefore function as proxy for each algal
682 taxon's relative abundance and potentially offer insights into feeding patterns for the grazers.

683

684 *Relating sewage indicators with macroinvertebrate feeding guilds*

685 In assessing benthic consumer communities' responses to changing periphyton, our data suggest
686 macroinvertebrate guilds reshape with increasing sewage pollution. Our results support the
687 general conclusion of Timoshkin et al. (2016) that Baikalian mollusk abundance tends to
688 decrease with increasing sewage pollution. Decreased mollusk abundance may have several
689 causes, including low tolerance for increased concentrations of PPCPs or other components of
690 sewage (e.g., Hollingsworth et al. 2002, Timoshkin et al. 2016), inability to consume filamentous
691 algae (Mazzella and Russo 1989), or filamentous algae not offering the proper nutrition (Lowe
692 and Hunter 1988). In contrast to mollusks, amphipods were generally prevalent at all littoral
693 sites, regardless of sewage indicator concentrations. *Brandtia* spp. was the only amphipod genus

694 less abundant with sewage indicator signals. This genus tends to be associated with endemic
695 sponges (Taakhteev & Didorenko, 2015), which may also be decreasing in abundance near areas
696 of lakeside development (Timoshkin et al., 2016). *Eulimnogammarus* spp., one of the most
697 speciose Baikal genera (Takhteev and Didorenko 2015), was prevalent at all sites, and $\delta^{15}\text{N}$
698 values in its tissue increased slightly but significantly with increasing IDW population. Unlike
699 periphyton, amphipods' increasing $\delta^{15}\text{N}$ values may relate to amphipods having longer cellular
700 turnover rates (e.g., weeks; McIntyre and Flecker 2006) relative to periphyton. Consequently,
701 amphipods' enhanced $\delta^{15}\text{N}$ values suggest that sewage-derived nutrients are being incorporated
702 into the food web. While we did not test amphipod tissues for other sewage indicators such as
703 PPCPs and microplastics, the potential for PPCPs to bioaccumulate and biomagnify in food webs
704 has been recently demonstrated, with ecological ramifications remaining uncertain (Lagesson et
705 al., 2016; Richmond et al., 2018). These combined results suggest that mollusk abundance and
706 amphipod $\delta^{15}\text{N}$ values may be longer-term indicators of sewage pollution in Baikal.

707

708 In contrast to variation in $\delta^{15}\text{N}$ values, amphipod fatty acid profiles did not differ markedly
709 between sites (Figure 7). Amphipods from all collected sites expressed consistent 20:5 ω 3
710 signatures relative to 18:3 ω 3 and 18:2 ω 6. Consumers usually accumulate fatty acids from their
711 food source. Yoshii's (1999) study as well as our own stable isotope data suggest that Baikal's
712 benthic, littoral amphipods are likely a combination of grazers and omnivores. Because fatty acid
713 profiles in amphipods largely reflected fatty acid signatures in periphyton, our data suggest that
714 amphipods likely continue grazing on periphyton, despite the food resource changing in
715 community composition and nutritional content. As a consequence, amphipods may be
716 compensating for the shifting nutritional quality of periphyton through at least two potential

717 mechanisms. First, amphipods may selectively consume diatoms as opposed to filamentous
718 algae, meaning diatom relative abundance could decrease both from increased grazing and lesser
719 efficiency at taking up nutrients relative to filamentous taxa. Second, amphipods themselves
720 (e.g., Desvilelettes et al. 1997; Castell et al. 2004) or heterotrophic symbionts (Klein Breteler et al.
721 1999; Veloza et al. 2006; Hiltunen et al. 2017) may upgrade fatty acids by investing energy to
722 convert C18 fatty acids to C20 fatty acids. Regardless of the exact mechanism, our data suggest
723 that food web interactions would change with increasing sewage pollution and may imply a net
724 energetic cost through amphipods' differential grazing patterns.

725

726 *Conclusions*

727 Over the past decade, Lake Baikal has shown signs of nearshore eutrophication, despite the
728 pelagic zone remaining ultra-oligotrophic. While Baikal receives nutrients from multiple sources,
729 sewage-specific indicators used in this study implicate wastewater pollution as one of the
730 sources. Our results corroborate work by Timoshkin et al. (2016, 2018), demonstrating how
731 patchy hot spots of lakeside development at Baikal can create gradients in sewage concentrations
732 and ecological responses. Unlike previous studies, our approach pairs community abundance
733 data (i.e., periphyton and macroinvertebrate counts) and nuanced dietary tracers (i.e., fatty acids)
734 to assess benthic community and food web consequences of sewage pollution. While sewage
735 pollution may lead to changing resources for macroinvertebrate grazers, Baikal's amphipods
736 appear to be compensating either (1) by selectively grazing on diatoms or (2) by consuming less
737 desirable food and upgrading fatty acids. In both cases, our results suggest shifting community
738 interactions and may imply a net energetic cost for amphipods, as they expend energy either by
739 foraging selectively for diatoms or by catabolizing certain essential fatty acids.

740

741 *Future trajectories: a call for increased nearshore monitoring*

742 Our results underscore the importance of nearshore monitoring in detecting sewage pollution in
743 large lakes. Lake Baikal is considered ultra-oligotrophic based on pelagic sampling (Yoshida et
744 al. 2003; O'Donnell et al. 2017), but nearshore hot spots of eutrophication are developing
745 throughout the lake (Timoshkin et al. 2016, 2018). While pelagic samples are representative of
746 the lake's overall status, nearshore sampling aids managers in identifying pollution loading
747 before the entire system is affected (Jacoby et al. 1991; Lambert et al. 2008; Hampton et al.
748 2011). Beyond Baikal, several large, deep, oligotrophic lakes have likewise experienced
749 localized sewage pollution with nearshore biological responses, despite pelagic measurements
750 suggesting oligotrophic status (e.g., Jacoby et al. 1991, Rosenberger et al. 2008; Hampton et al.,
751 2011). Once eutrophication of the open water has occurred, mitigation can involve complex
752 socio-economic factors (Carpenter et al. 1999), require system-specific information (Jeppesen et
753 al. 2005), and necessitate long-term strategies (Tong et al. 2020). Because nutrients may enter
754 systems from numerous sources, incorporating sewage specific indicators, such as PPCPs, may
755 be necessary. PPCP sampling has the potential to not only identify sewage-associated nutrient
756 pollution but also assess heterogeneities in sewage loading along a shoreline. When PPCP data
757 are paired with co-located benthic community composition and food web data, managers can
758 take system-specific actions to mitigate ecological consequences before sewage concentrations
759 are detected throughout the lake. Across larger spatial and temporal scales, these paired PPCP-
760 biological samples have potential to offer a synoptic view of the impacts of sewage pollution,
761 enabling regional and local monitoring to coordinate mitigation strategies

762

763

764

Works Cited

765 Anderson, M. J. 2001. A new method for non-parametric multivariate analysis of variance. *Austral*

766 *Ecology* **26**: 32–46. doi:10.1111/j.1442-9993.2001.01070.pp.x

767 Andersson, E., and A.-K. Brunberg. 2006. Inorganic nutrient acquisition in a shallow clearwater lake –

768 dominance of benthic microbiota. *Aquatic Sciences* **68**: 172–180. doi:10.1007/s00027-006-0805-

769 x

770 Anisimov, O., and S. Reneva. 2006. Permafrost and Changing Climate: The Russian Perspective. *Ambio*

771 **35**: 169–175.

772 Barnes, D. K. A., F. Galgani, R. C. Thompson, and M. Barlaz. 2009. Accumulation and fragmentation of
773 plastic debris in global environments. *Philos Trans R Soc Lond B Biol Sci* **364**: 1985–1998.

774 doi:10.1098/rstb.2008.0205

775 Bendz, D., N. A. Paxéus, T. R. Ginn, and F. J. Loge. 2005. Occurrence and fate of pharmaceutically
776 active compounds in the environment, a case study: Höje River in Sweden. *Journal of Hazardous
777 Materials* **122**: 195–204. doi:10.1016/j.jhazmat.2005.03.012

778 Brandon, J. A., A. Freibott, and L. M. Sala. 2020. Patterns of suspended and salp-ingested microplastic
779 debris in the North Pacific investigated with epifluorescence microscopy. *Limnology and
780 Oceanography Letters* **5**: 46–53. doi:10.1002/ol.2.10127

781 Brandon, J., M. Goldstein, and M. D. Ohman. 2016. Long-term aging and degradation of microplastic
782 particles: Comparing in situ oceanic and experimental weathering patterns. *Marine Pollution
783 Bulletin* **110**: 299–308. doi:10.1016/j.marpolbul.2016.06.048

784 Brodin, T., J. Fick, M. Jonsson, and J. Klaminder. 2013. Dilute concentrations of a psychiatric drug alter
785 behavior of fish from natural populations. *Science* **339**: 814–815. doi:10.1126/science.1226850

- 786 Camilleri, A. C., and T. Ozersky. 2019. Large variation in periphyton $\delta^{13}\text{C}$ and $\delta^{15}\text{N}$ values in the upper
787 Great Lakes: Correlates and implications. *Journal of Great Lakes Research* **45**: 986–990.
788 doi:10.1016/j.jglr.2019.06.003
- 789 Carpenter, S. R., D. Ludwig, and W. A. Brock. 1999. Management of eutrophication for lakes subject to
790 potentially irreversible change. *Ecological Applications* **9**: 751–771. doi:10.2307/2641327
- 791 Castell, J. D., E. J. Kennedy, S. M. C. Robinson, G. J. Parsons, T. J. Blair, and E. Gonzalez-Duran. 2004.
792 Effect of dietary lipids on fatty acid composition and metabolism in juvenile green sea urchins
793 (*Strongylocentrotus droebachiensis*). *Aquaculture* **242**: 417–435.
794 doi:10.1016/j.aquaculture.2003.11.003
- 795 Chang, H.-Y., S.-H. Wu, K.-T. Shao, and others. 2012. Longitudinal variation in food sources and their
796 use by aquatic fauna along a subtropical river in Taiwan. *Freshwater Biology* **57**: 1839–1853.
797 doi:10.1111/j.1365-2427.2012.02843.x
- 798 Clarke, K. R. 1993. Non-parametric multivariate analyses of changes in community structure. *Australian
799 Journal of Ecology* **18**: 117–143. doi:<https://doi.org/10.1111/j.1442-9993.1993.tb00438.x>
- 800 Cole, M. L., I. Valiela, K. D. Kroeger, and others. 2004. Assessment of a $\delta^{15}\text{N}$ isotopic method to indicate
801 anthropogenic eutrophication in aquatic ecosystems. *J. Environ. Qual.* **33**: 124–132.
802 doi:10.2134/jeq2004.1240
- 803 Costanzo, S. D., M. J. O'Donohue, W. C. Dennison, N. R. Loneragan, and M. Thomas. 2001. A new
804 approach for detecting and mapping sewage impacts. *Marine Pollution Bulletin* **42**: 149–156.
805 doi:10.1016/S0025-326X(00)00125-9
- 806 Craine, J. M., A. J. Elmore, L. Wang, and others. 2018. Isotopic evidence for oligotrophication of
807 terrestrial ecosystems. *Nature Ecology & Evolution* **2**: 1735–1744. doi:10.1038/s41559-018-
808 0694-0
- 809 Czekalski, N., R. Sigdel, J. Birtel, B. Matthews, and H. Bürgmann. 2015. Does human activity impact the
810 natural antibiotic resistance background? Abundance of antibiotic resistance genes in 21 Swiss
811 lakes. *Environment International* **81**: 45–55. doi:10.1016/j.envint.2015.04.005

- 812 D'Alessio, M., S. Onanong, D. D. Snow, and C. Ray. 2018. Occurrence and removal of pharmaceutical
813 compounds and steroids at four wastewater treatment plants in Hawai'i and their environmental
814 fate. *Science of The Total Environment* **631–632**: 1360–1370.
815 doi:10.1016/j.scitotenv.2018.03.100
- 816 Dalsgaard, J., M. St. John, G. Kattner, D. Müller-Navarra, and W. Hagen. 2003. Fatty acid trophic
817 markers in the pelagic marine environment, p. 225–340. *In Advances in Marine Biology*.
818 Elsevier.
- 819 Desvilettes, Ch., G. Bourdier, and J. Ch. Breton. 1997. On the occurrence of a possible bioconversion of
820 linolenic acid into docosahexaenoic acid by the copepod *Eucyclops serrulatus* fed on microalgae.
821 *J Plankton Res* **19**: 273–278. doi:10.1093/plankt/19.2.273
- 822 Dziewczynski, T. L., B. A. Campbell, and J. L. Kane. 2016. Dose-dependent fluoxetine effects on
823 boldness in male Siamese fighting fish. *Journal of Experimental Biology* **219**: 797–804.
824 doi:10.1242/jeb.132761
- 825 Eerkes-Medrano, D., R. C. Thompson, and D. C. Aldridge. 2015. Microplastics in freshwater systems: A
826 review of the emerging threats, identification of knowledge gaps and prioritisation of research
827 needs. *Water Research* **75**: 63–82. doi:10.1016/j.watres.2015.02.012
- 828 Eriksen, M., S. Mason, S. Wilson, C. Box, A. Zellers, W. Edwards, H. Farley, and S. Amato. 2013.
829 Microplastic pollution in the surface waters of the Laurentian Great Lakes. *Marine Pollution
830 Bulletin* **77**: 177–182. doi:10.1016/j.marpolbul.2013.10.007
- 831 Feijão, E., R. Cruz de Carvalho, I. A. Duarte, and others. 2020. Fluoxetine arrests growth of the model
832 diatom *Phaeodactylum tricornutum* by increasing oxidative stress and altering energetic and lipid
833 metabolism. *Front Microbiol* **11**. doi:10.3389/fmicb.2020.01803
- 834 Fellows, I., and using the Jm. library by J. P. Stotz. 2019. OpenStreetMap: Access to Open Street Map
835 Raster Images,.
- 836 Firke, S. 2020. janitor: Simple Tools for Examining and Cleaning Dirty Data.

- 837 Fischer, E. K., L. Paglia longa, E. Czech, and M. Tamminga. 2016. Microplastic pollution in lakes and
838 lake shoreline sediments – A case study on Lake Bolsena and Lake Chiusi (central Italy).
839 Environmental Pollution **213**: 648–657. doi:10.1016/j.envpol.2016.03.012
- 840 Focazio, M. J., D. W. Kolpin, K. K. Barnes, E. T. Furlong, M. T. Meyer, S. D. Zaugg, L. B. Barber, and
841 M. E. Thurman. 2008. A national reconnaissance for pharmaceuticals and other organic
842 wastewater contaminants in the United States - II) Untreated drinking water sources. Science of
843 the Total Environment **402**: 201–216. doi:10.1016/j.scitotenv.2008.02.021
- 844 Free, C. M., O. P. Jensen, S. A. Mason, M. Eriksen, N. J. Williamson, and B. Boldgiv. 2014. High-levels
845 of microplastic pollution in a large, remote, mountain lake. Marine Pollution Bulletin **85**: 156–
846 163. doi:10.1016/j.marpolbul.2014.06.001
- 847 Galloway, A. W. E., and M. Winder. 2015. Partitioning the relative importance of phylogeny and
848 environmental conditions on phytoplankton fatty acids. PLOS ONE **10**: e0130053.
849 doi:10.1371/journal.pone.0130053
- 850 Galloway, J. N., F. J. Dentener, D. G. Capone, and others. 2004. Nitrogen cycles: Past, present, and
851 future. biogeochemistry **70**: 153–226. doi:10.1007/s10533-004-0370-0
- 852 Garnier, S. 2018. viridis: Default Color Maps from “matplotlib.”
- 853 Gartner, A., P. Lavery, and A. J. Smit. 2002. Use of $\delta^{15}\text{N}$ signatures of different functional forms of
854 macroalgae and filter-feeders to reveal temporal and spatial patterns in sewage dispersal. Mar.
855 Ecol.-Prog. Ser. **235**: 63–73. doi:10.3354/meps235063
- 856 Green, D. S. 2016. Effects of microplastics on European flat oysters, *Ostrea edulis* and their associated
857 benthic communities. Environmental Pollution **216**: 95–103. doi:10.1016/j.envpol.2016.05.043
- 858 Guzzo, M. M., G. D. Haffner, S. Sorge, S. A. Rush, and A. T. Fisk. 2011. Spatial and temporal
859 variabilities of $\delta^{13}\text{C}$ and $\delta^{15}\text{N}$ within lower trophic levels of a large lake: implications for
860 estimating trophic relationships of consumers. Hydrobiologia **675**: 41–53. doi:10.1007/s10750-
861 011-0794-1

- 862 Hadwen, W. L., and S. E. Bunn. 2005. Food web responses to low-level nutrient and $\delta^{15}\text{N}$ -tracer additions
863 in the littoral zone of an oligotrophic dune lake. *Limnology and Oceanography* **50**: 1096.
- 864 Hampton, S. E., S. C. Fradkin, P. R. Leavitt, and E. E. Rosenberger. 2011. Disproportionate importance
865 of nearshore habitat for the food web of a deep oligotrophic lake. *Marine and Freshwater
866 Research* **62**: 350. doi:10.1071/MF10229
- 867 Hampton, S. E., S. McGowan, T. Ozersky, and others. 2018. Recent ecological change in ancient lakes.
868 *Limnology and Oceanography* **63**: 2277–2304. doi:10.1002/lno.10938
- 869 Hanvey, J. S., P. J. Lewis, J. L. Lavers, N. D. Crosbie, K. Pozo, and B. O. Clarke. 2017. A review of
870 analytical techniques for quantifying microplastics in sediments. *Anal. Methods* **9**: 1369–1383.
871 doi:10.1039/C6AY02707E
- 872 Hendrickson, E., E. C. Minor, and K. Schreiner. 2018. Microplastic abundance and composition in
873 western lake superior as determined via microscopy, Pyr-GC/MS, and FTIR. *Environ. Sci.
874 Technol.* **52**: 1787–1796. doi:10.1021/acs.est.7b05829
- 875 Hester, J., and H. Wickham. 2019. fs: Cross-Platform File System Operations Based on “libuv.”
- 876 Hiltunen, M., M. Honkanen, S. Taipale, U. Strandberg, and P. Kankaala. 2017. Trophic upgrading via the
877 microbial food web may link terrestrial dissolved organic matter to Daphnia. *J Plankton Res* **39**:
878 861–869. doi:10.1093/plankt/fbx050
- 879 Hollingsworth, R. G., J. W. Armstrong, and E. Campbell. 2002. Caffeine as a repellent for slugs and
880 snails. *Nature* **417**: 915–916. doi:10.1038/417915a
- 881 Interfax-Tourism. 2018. Байкал с января по август 2018 года посетили 1,2 миллиона туристов (1.2
882 million tourists visited Baikal from January through August 2018). Interfax-Tourism, October 25
- 883 Iverson, S. J., C. Field, W. D. Bowen, and W. Blanchard. 2004. Quantitative Fatty Acid Signature
884 Analysis: A New Method of Estimating Predator Diets. *Ecological Monographs* **74**: 211–235.
885 doi:10.1890/02-4105
- 886 Izhboldina, L. A. 2007. Guide and Key to Benthic and Periphyton Algae of Lake Baikal (meio- and
887 macrophytes) with Brief Notes on Their Ecology, Nauka-Centre.

- 888 Jacoby, J. M., D. D. Bouchard, and C. R. Patmont. 1991. Response of periphyton to nutrient enrichment
889 in Lake Chelan, WA. *Lake and Reservoir Management* **7**: 33–43.
890 doi:10.1080/07438149109354252
- 891 Jeppesen, E., M. Søndergaard, J. P. Jensen, and others. 2005. Lake responses to reduced nutrient loading
892 – an analysis of contemporary long-term data from 35 case studies. *Freshwater Biology* **50**:
893 1747–1771. doi:10.1111/j.1365-2427.2005.01415.x
- 894 Johnson, R. A., and D. V. Wichern. 2007. *Applied Multivariate Statistical Analysis*, 6th ed. Prentice Hall.
- 895 Karnaukhov, D., S. Biritskaya, E. Dolinskaya, M. Teplykh, N. Silenko, Y. Ermolaeva, and E. Silow.
896 2020. Pollution by macro- and microplastic of large lacustrine ecosystems in eastern Asia.
897 *Pollution Research* **2**: 353–355.
- 898 Karnjanapiboonwong, A., A. N. Morse, J. D. Maul, and T. A. Anderson. 2010. Sorption of estrogens,
899 triclosan, and caffeine in a sandy loam and a silt loam soil. *Journal of Soils and Sediments* **10**:
900 1300–1307. doi:10.1007/s11368-010-0223-5
- 901 Kassambara, A. 2019. *ggpubr: “ggplot2” Based Publication Ready Plots*,
902 Kassambara, A., and F. Mundt. 2019. *factoextra: Extract and Visualize the Results of Multivariate Data*
903 *Analyses*,
904 Kaufman, L., and P. J. Rousseeuw. 2005. *Finding Groups in Data: An Introduction to Cluster Analysis*,
905 1st Edition. Wiley-Interscience.
906 Kelly, J. R., and R. E. Scheibling. 2012. Fatty acids as dietary tracers in benthic food webs. *Marine*
907 *Ecology Progress Series* **446**: 1–22. doi:10.3354/meps09559
908 Klein Breteler, W. C. M., N. Schogt, M. Baas, S. Schouten, and G. W. Kraay. 1999. Trophic upgrading of
909 food quality by protozoans enhancing copepod growth: role of essential lipids. *Marine Biology*
910 **135**: 191–198. doi:10.1007/s002270050616
911 Klein, S., E. Worch, and T. P. Knepper. 2015. Occurrence and spatial distribution of microplastics in river
912 shore sediments of the Rhine-Main area in Germany. *Environ. Sci. Technol.* **49**: 6070–6076.
913 doi:10.1021/acs.est.5b00492

- 914 Kolpin, D. W., E. T. Furlong, M. T. Meyer, E. M. Thurman, S. D. Zaugg, L. B. Barber, and H. T. Buxton.
- 915 2002. Pharmaceuticals, hormones, and other organic wastewater contaminants in u.s. streams,
- 916 1999–2000: A national reconnaissance. *Environmental Science & Technology* **36**: 1202–1211.
- 917 doi:10.1021/es011055j
- 918 Kozhov, M. M. 1963. *Lake Baikal and its Life*, Springer Science & Business Media.
- 919 Kozhova, O. M., and L. R. Izmest'eva. 1998. *Lake Baikal: Evolution and Biodiversity*, Backhuys
- 920 Publishers.
- 921 Kravtsova, L. S., L. A. Izhboldina, I. V. Khanaev, and others. 2014. Nearshore benthic blooms of
- 922 filamentous green algae in Lake Baikal. *Journal of Great Lakes Research* **40**: 441–448.
- 923 doi:10.1016/j.jglr.2014.02.019
- 924 Lagesson, A., J. Fahlman, T. Brodin, J. Fick, M. Jonsson, P. Byström, and J. Klaminder. 2016.
- 925 Bioaccumulation of five pharmaceuticals at multiple trophic levels in an aquatic food web -
- 926 Insights from a field experiment. *Science of The Total Environment* **568**: 208–215.
- 927 doi:10.1016/j.scitotenv.2016.05.206
- 928 Lambert, D., A. Cattaneo, and R. Carignan. 2008. Periphyton as an early indicator of perturbation in
- 929 recreational lakes. *Can. J. Fish. Aquat. Sci.* **65**: 258–265. doi:10.1139/f07-168
- 930 Legendre, P., and L. Legendre. 2012. *Numerical Ecology*, 3rd ed. Elsevier.
- 931 Li, J., C. Green, A. Reynolds, H. Shi, and J. M. Rotchell. 2018. Microplastics in mussels sampled from
- 932 coastal waters and supermarkets in the United Kingdom. *Environmental Pollution* **241**: 35–44.
- 933 doi:10.1016/j.envpol.2018.05.038
- 934 Lorenzen, C. J. 1967. Determination of chlorophyll and pheo-pigments: Spectrophotometric equations1.
- 935 Limnology and Oceanography **12**: 343–346. doi:<https://doi.org/10.4319/lo.1967.12.2.0343>
- 936 Lowe, R. L., and R. D. Hunter. 1988. Effect of grazing by *Physa integra* on periphyton community
- 937 structure. *Journal of the North American Benthological Society* **7**: 29–36. doi:10.2307/1467828
- 938 Maechler, M., P. Rousseeuw, A. Struyf, M. Hubert, and K. Hornik. 2019. *cluster: Cluster Analysis Basics*
- 939 and Extensions,

- 940 Mazzella, L., and G. F. Russo. 1989. Grazing effect of two *Gibbula* species (Mollusca,
941 Archaeogastropoda) on the epiphytic community of *Posidonia oceanica* leaves.
- 942 McIntyre, P. B., and A. S. Flecker. 2006. Rapid turnover of tissue nitrogen of primary consumers in
943 tropical freshwaters. *Oecologia* **148**: 12–21. doi:10.1007/s00442-005-0354-3
- 944 Meyer, M. F., T. Ozersky, K. H. Woo, and others. 2020. A unified dataset of co-located sewage pollution,
945 periphyton, and benthic macroinvertebrate community and food web structure from Lake Baikal
946 (Siberia).doi:10.6073/PASTA/76F43144015EC795679BAC508EFA044B
- 947 Meyer, M. F., S. M. Powers, and S. E. Hampton. 2019. An evidence synthesis of pharmaceuticals and
948 personal care products (PPCPs) in the environment: Imbalances among compounds, sewage
949 treatment techniques, and ecosystem types. *Environ. Sci. Technol.* **53**: 12961–12973.
950 doi:10.1021/acs.est.9b02966
- 951 Meyer, M., T. Ozersky, K. Woo, A. W. E. Galloway, M. R. Brousil, and S. Hampton. 2015. Baikal Food
952 Webs. doi:10.17605/OSF.IO/9TA8Z
- 953 Monteith, D. T., J. L. Stoddard, C. D. Evans, and others. 2007. Dissolved organic carbon trends resulting
954 from changes in atmospheric deposition chemistry. *Nature* **450**: 537–540.
955 doi:10.1038/nature06316
- 956 Moore, J. W., D. E. Schindler, M. D. Scheuerell, D. Smith, and J. Frogge. 2003. Lake eutrophication at
957 the urban fringe, Seattle region, USA. *AMBIO: A Journal of the Human Environment* **32**: 13–18.
- 958 Moore, M. V., S. E. Hampton, L. R. Izmest'eva, E. A. Silow, E. V. Peshkova, and B. K. Pavlov. 2009.
959 Climate Change and the World's "Sacred Sea"-Lake Baikal, Siberia. *Bioscience* **59**: 405–417.
960 doi:10.1525/bio.2009.59.5.8
- 961 Moran, P. W., S. E. Cox, S. S. Embrey, R. L. Huffman, T. D. Olsen, and S. C. Fradkin. 2012. Sources and
962 Sinks of Nitrogen and Phosphorus in a Deep, Oligotrophic Lake, Lake Crescent, Olympic
963 National Park, Washington. US Geological Survey.
- 964 O'Donnell, D. R., P. Wilburn, E. A. Silow, L. Y. Yampolsky, and E. Litchman. 2017. Nitrogen and
965 phosphorus colimitation of phytoplankton in Lake Baikal: Insights from a spatial survey and

- 966 nutrient enrichment experiments. *Limnology and Oceanography* **62**: 1383–1392.
- 967 doi:10.1002/lno.10505
- 968 Oksanen, J., F. G. Blanchet, M. Friendly, and others. 2019. *vegan: Community Ecology Package*,
- 969 Osipova, S., L. Dudareva, N. Bondarenko, A. Nasarova, N. Sokolova, L. Obolkina, O. Glyzina, and O.
- 970 Timoshkin. 2009. Temporal variation in fatty acid composition of *Ulothrix zonata* (Chlorophyta)
- 971 from ice and benthic communities of Lake Baikal. *Phycologia* **48**: 130–135.
- 972 Ozersky, T., E. A. Volkova, N. A. Bondarenko, O. A. Timoshkin, V. V. Malnik, V. M. Domysheva, and
- 973 S. E. Hampton. 2018. Nutrient limitation of benthic algae in Lake Baikal, Russia. *Freshwater*
- 974 *Science* **37**: 472–482. doi:10.1086/699408
- 975 Parsons, T. R., and J. D. H. Strickland. 1963. Discussion of spectrophotometric determination of marine-
- 976 plant pigments, with revised equations for ascertaining chlorophylls and carotenoids. *Journal of*
- 977 *Marine Research*.
- 978 Pebesma, E. 2018. Simple Features for R: Standardized Support for Spatial Vector Data. *The R Journal*
- 979 **10**: 439–446. doi:10.32614/RJ-2018-009
- 980 Piñón-Gimate, A., M. F. Soto-Jiménez, M. J. Ochoa-Izaguirre, E. García-Pagés, and F. Páez-Osuna. 2009.
- 981 Macroalgae blooms and $\delta^{15}\text{N}$ in subtropical coastal lagoons from the Southeastern Gulf of
- 982 California: Discrimination among agricultural, shrimp farm and sewage effluents. *Marine*
- 983 *Pollution Bulletin* **58**: 1144–1151. doi:10.1016/j.marpolbul.2009.04.004
- 984 Powers, S. M., T. W. Bruulsema, T. P. Burt, and others. 2016. Long-term accumulation and transport of
- 985 anthropogenic phosphorus in three river basins. *Nature Geoscience* **9**: 353–356.
- 986 doi:10.1038/ngeo2693
- 987 R Core Team. 2019. *R: A Language and Environment for Statistical Computing*,
- 988 del Rey, Z. R., E. F. Granek, and B. A. Buckley. 2011. Expression of HSP70 in *Mytilus californianus*
- 989 following exposure to caffeine. *Ecotoxicology* **20**: 855–861. doi:10.1007/s10646-011-0649-6
- 990 Richmond, E. K., E. J. Rosi, A. J. Reisinger, B. R. Hanrahan, R. M. Thompson, and M. R. Grace. 2019.
- 991 Influences of the antidepressant fluoxetine on stream ecosystem function and aquatic insect

- 992 emergence at environmentally realistic concentrations. *Journal of Freshwater Ecology* **34**: 513–
993 531. doi:10.1080/02705060.2019.1629546
- 994 Richmond, E. K., E. J. Rosi, D. M. Walters, J. Fick, S. K. Hamilton, T. Brodin, A. Sundelin, and M. R.
995 Grace. 2018. A diverse suite of pharmaceuticals contaminates stream and riparian food webs.
996 *Nature Communications* **9**: 4491. doi:10.1038/s41467-018-06822-w
- 997 Risk, M. J., B. E. Lapointe, O. A. Sherwood, and B. J. Bedford. 2009. The use of $\delta^{15}\text{N}$ in assessing
998 sewage stress on coral reefs. *Marine Pollution Bulletin* **58**: 793–802.
999 doi:10.1016/j.marpolbul.2009.02.008
- 1000 Robson, S. V., E. J. Rosi, E. K. Richmond, and M. R. Grace. 2020. Environmental concentrations of
1001 pharmaceuticals alter metabolism, denitrification, and diatom assemblages in artificial streams.
1002 *Freshwater Science* **39**: 256–267. doi:10.1086/708893
- 1003 Romera-Castillo, C., M. Pinto, T. M. Langer, X. A. Álvarez-Salgado, and G. J. Herndl. 2018. Dissolved
1004 organic carbon leaching from plastics stimulates microbial activity in the ocean. *Nat Commun* **9**:
1005 1–7. doi:10.1038/s41467-018-03798-5
- 1006 Rosenberger, E. E., S. E. Hampton, S. C. Fradkin, and B. P. Kennedy. 2008. Effects of shoreline
1007 development on the nearshore environment in large deep oligotrophic lakes. *Freshwater Biology*
1008 **53**: 1673–1691. doi:10.1111/j.1365-2427.2008.01990.x
- 1009 Rosi-Marshall, E. J., D. W. Kincaid, H. A. Bechtold, T. V. Royer, M. Rojas, and J. J. Kelly. 2013.
1010 Pharmaceuticals suppress algal growth and microbial respiration and alter bacterial communities
1011 in stream biofilms. *Ecological Applications* **23**: 583–593. doi:10.1890/12-0491.1
- 1012 Rosi-Marshall, E. J., and T. V. Royer. 2012. Pharmaceutical compounds and ecosystem function: An
1013 emerging research challenge for aquatic ecologists. *Ecosystems* **15**: 867–880.
1014 doi:10.1007/s10021-012-9553-z
- 1015 Sargent, J. R., and S. Falk-Petersen. 1988. The lipid biochemistry of calanoid copepods. *Hydrobiologia*
1016 **167–168**: 101–114. doi:10.1007/BF00026297

- 1017 Savage, C., and R. Elmgren. 2004. Macroalgal (*Fucus vesiculosus*) $\delta^{15}\text{N}$ values trace decrease in sewage
1018 influence. *Ecological Applications* **14**: 517–526. doi:10.1890/02-5396
- 1019 Schram, J. B., J. N. Kobelt, M. N. Dethier, and A. W. E. Galloway. 2018. Trophic transfer of macroalgal
1020 fatty acids in two urchin species: Digestion, egestion, and tissue building. *Front. Ecol. Evol.* **6**.
1021 doi:10.3389/fevo.2018.00083
- 1022 Shishlyannikov, S. M., A. A. Nikonova, Y. S. Bukin, and A. G. Gorshkov. 2018. Fatty acid trophic
1023 markers in Lake Baikal phytoplankton: A comparison of endemic and cosmopolitan diatom-
1024 dominated phytoplankton assemblages. *Ecological Indicators* **85**: 878–886.
1025 doi:10.1016/j.ecolind.2017.11.052
- 1026 Sitnikova, T. Ya. 2012. Определитель брюхоногих моллюсков бухты Большие Коты (юго-западное
1027 побережье озера Байкал) [Key of the Gastropod Molluscs in the Bay of Bolshie Koty (South-
1028 West shoreline of Lake Baikal)], Irkutsk State University.
- 1029 Slowikowski, K. 2019. ggrepel: Automatically Position Non-Overlapping Text Labels with “ggplot2.”
- 1030 Smith, V. H., G. D. Tilman, and J. C. Nekola. 1999. Eutrophication: Impacts of excess nutrient inputs on
1031 freshwater, marine, and terrestrial ecosystems. *Environmental Pollution* **100**: 179–196.
1032 doi:10.1016/S0269-7491(99)00091-3
- 1033 Sneath, P. H. A., and R. R. Sokal. 1973. Numerical Taxonomy: The Principles and Practice of Numerical
1034 Classification, W. H. Freeman.
- 1035 Steinmetz, Z., C. Wollmann, M. Schaefer, and others. 2016. Plastic mulching in agriculture: Trading
1036 short-term agronomic benefits for long-term soil degradation? *Science of The Total Environment*
1037 **550**: 690–705. doi:10.1016/j.scitotenv.2016.01.153
- 1038 Stoddard, J. L., J. Van Sickle, A. T. Herlihy, J. Brahney, S. Paulsen, D. V. Peck, R. Mitchell, and A. I.
1039 Pollard. 2016. Continental-scale increase in lake and stream phosphorus: Are oligotrophic
1040 systems disappearing in the united states? *Environ. Sci. Technol.* **50**: 3409–3415.
1041 doi:10.1021/acs.est.5b05950
- 1042 Sumner, M. D. 2019. spdpqr: Data Manipulation Verbs for the Spatial Classes,.

- 1043 Suzuki, R., Y. Terada, and H. Shimodaira. 2019. *pvclust*: Hierarchical Clustering with P-Values via
1044 Multiscale Bootstrap Resampling.,
- 1045 Swamikannu, X., and K. D. Hoagland. 1989. Effects of snail grazing on the diversity and structure of a
1046 periphyton community in a eutrophic pond. *Can. J. Fish. Aquat. Sci.* **46**: 1698–1704.
1047 doi:10.1139/f89-215
- 1048 Swann, G. E. A., V. N. Panizzo, S. Piccolroaz, and others. 2020. Changing nutrient cycling in Lake
1049 Baikal, the world's oldest lake. *PNAS* **117**: 27211–27217. doi:10.1073/pnas.2013181117
- 1050 Taipale, S., U. Strandberg, E. Peltomaa, A. W. E. Galloway, A. Ojala, and M. T. Brett. 2013. Fatty acid
1051 composition as biomarkers of freshwater microalgae: Analysis of 37 strains of microalgae in 22
1052 genera and in seven classes. *Aquatic Microbial Ecology* **71**: 165–178. doi:10.3354/ame01671
- 1053 Takhteev, V. V., and D. I. Didorenko. 2015. Fauna and ecology of amphipods of Lake Baikal: A Training
1054 manual, V.B. Sochava Institute of Geography SB RAS.
- 1055 Timoshkin, O. A., M. V. Moore, N. N. Kulikova, and others. 2018. Groundwater contamination by
1056 sewage causes benthic algal outbreaks in the littoral zone of Lake Baikal (East Siberia). *Journal*
1057 *of Great Lakes Research*. doi:10.1016/j.jglr.2018.01.008
- 1058 Timoshkin, O. A., D. P. Samsonov, M. Yamamoto, and others. 2016. Rapid ecological change in the
1059 coastal zone of Lake Baikal (East Siberia): Is the site of the world's greatest freshwater
1060 biodiversity in danger? *Journal of Great Lakes Research* **42**: 487–497.
1061 doi:10.1016/j.jglr.2016.02.011
- 1062 Tong, Y., M. Wang, J. Peñuelas, and others. 2020. Improvement in municipal wastewater treatment alters
1063 lake nitrogen to phosphorus ratios in populated regions. *Proc Natl Acad Sci USA* **117**: 11566–
1064 11572. doi:10.1073/pnas.1920759117
- 1065 Tornqvist, R., J. Jarsjo, J. Pietron, A. Bring, P. Rogberg, S. M. Asokan, and G. Destouni. 2014. Evolution
1066 of the hydro-climate system in the Lake Baikal basin. *Journal of Hydrology* **519**: 1953–1962.
1067 doi:10.1016/j.jhydrol.2014.09.074

- 1068 Turetsky, M. R., R. K. Wieder, C. J. Williams, and D. H. Vitt. 2000. Organic matter accumulation, peat
1069 chemistry, and permafrost melting in peatlands of boreal Alberta. *Écoscience* **7**: 115–122.
1070 doi:10.1080/11956860.2000.11682608
- 1071 Veloza, A. J., F.-L. E. Chu, and K. W. Tang. 2006. Trophic modification of essential fatty acids by
1072 heterotrophic protists and its effects on the fatty acid composition of the copepod *Acartia tonsa*.
1073 *Marine Biology* **148**: 779–788. doi:10.1007/s00227-005-0123-1
- 1074 Volkova, E. A., N. A. Bondarenko, and O. A. Timoshkin. 2018. Morphotaxonomy, distribution and
1075 abundance of *Spirogyra* (Zygnematophyceae, Charophyta) in Lake Baikal, East Siberia.
1076 *Phycologia* **57**: 298–308. doi:10.2216/17-69.1
- 1077 de Vries, J. 1972. Soil filtration of wastewater effluent and the mechanism of pore clogging. *Journal*
1078 (Water Pollution Control Federation) **44**: 565–573.
- 1079 Wang, W., and J. Wang. 2018. Investigation of microplastics in aquatic environments: An overview of
1080 the methods used, from field sampling to laboratory analysis. *TrAC Trends in Analytical*
1081 *Chemistry* **108**: 195–202. doi:10.1016/j.trac.2018.08.026
- 1082 Wayland, M., and K. A. Hobson. 2001. Stable carbon, nitrogen, and sulfur isotope ratios in riparian food
1083 webs on rivers receiving sewage and pulp-mill effluents. *Can. J. Zool.* **79**: 5–15. doi:10.1139/z00-
1084 169
- 1085 Wickham, H., M. Averick, J. Bryan, and others. 2019. Welcome to the tidyverse. *Journal of Open Source*
1086 Software **4**: 1686. doi:10.21105/joss.01686
- 1087 Wilke, C. O. 2019. *cowplot: Streamlined Plot Theme and Plot Annotations for “ggplot2,”*
- 1088 Wilke, C. O. 2020. *ggttext: Improved Text Rendering Support for “ggplot2,”*
- 1089 Yang, Y., W. Song, H. Lin, W. Wang, L. Du, and W. Xing. 2018. Antibiotics and antibiotic resistance
1090 genes in global lakes: A review and meta-analysis. *Environment International* **116**: 60–73.
1091 doi:10.1016/j.envint.2018.04.011

- 1092 Yang, Y.-Y., G. S. Toor, P. C. Wilson, and C. F. Williams. 2016. Septic systems as hot-spots of
1093 pollutants in the environment: Fate and mass balance of micropollutants in septic drainfields.
1094 *Science of The Total Environment* **566–567**: 1535–1544. doi:10.1016/j.scitotenv.2016.06.043
- 1095 York, J. K., G. Tomasky, I. Valiela, and D. J. Repeta. 2007. Stable isotopic detection of ammonium and
1096 nitrate assimilation by phytoplankton in the Waquoit Bay estuarine system. *Limnology and*
1097 *Oceanography* **52**: 144–155. doi:10.4319/lo.2007.52.1.0144
- 1098 Yoshida, T., T. Sekino, M. Genkai-Kato, and others. 2003. Seasonal dynamics of primary production in
1099 the pelagic zone of southern Lake Baikal. *Limnology* **4**: 53–62. doi:10.1007/s10201-002-0089-3
- 1100 Yoshii, K. 1999. Stable isotope analyses of benthic organisms in Lake Baikal. *Hydrobiologia* **411**: 145–
1101 159.
- 1102 2016a. Methods for determination of nitrogen-containing matters (with corrections) (Методы
1103 определения азотсодержащих веществ (с Поправками)).
- 1104 2016b. Methods for determination of phosphorus-containing matters (with corrections) (Методы
1105 определения фосфорсодержащих веществ).
- 1106 2017. Nitrate concentration in waters: Photometric methods with Giress reagent following stabilization in
1107 a cadmium reducer (Массовая концентрация нитратного азота в водах: Методика измерений
1108 фотометрическим методом с реагентом Грисса после восстановления в камиевом
1109 редукторе).
- 1110

1111 **Acknowledgments**

1112 We would like to thank the faculty, students, staff, and mariners of the Irkutsk State University's
1113 Biological Research Institute Biostation for their expert field, taxonomic, and laboratory support;
1114 Marianne Moore and Bart De Stasio for helpful advice; the researchers and students of the
1115 Siberian Branch of the Russian Academy of Sciences Limnological Institute for expert
1116 taxonomic and logistical assistance; Oleg A. Timoshkin, Tatiana Ya. Sitnikova, Irina V.
1117 Mekhanikova, Nina A. Bonderenko, Ekaterina Volkova, Yulia Zvereva, Vadim V. Takhteev,
1118 Stephanie G. Labou, Stephen L. Katz, Brian P. Lanouette, John R. Loffredo, Alli N. Cramer,
1119 Alexander K. Fremier, Erica J. Crespi, Stephen M. Powers, Daniel L. Preston, Gavin L.
1120 Simpson, and James J. Elser for offering insights throughout the development of this project.
1121 Funding was provided by the National Science Foundation (NSF-DEB-1136637) to S.E.H., a
1122 Fulbright Fellowship to M.F.M., a NSF Graduate Research Fellowship to M.F.M. (NSF-DGE-
1123 1347973), and the Russian Ministry of Science and Education (N FZZE-2020-0026; N FZZE-
1124 2020-0023). This work serves as one chapter of M.F.M.'s doctoral dissertation in Environmental
1125 and Natural Resource Sciences at Washington State University.

1126

1127 **Conflicts of Interest**

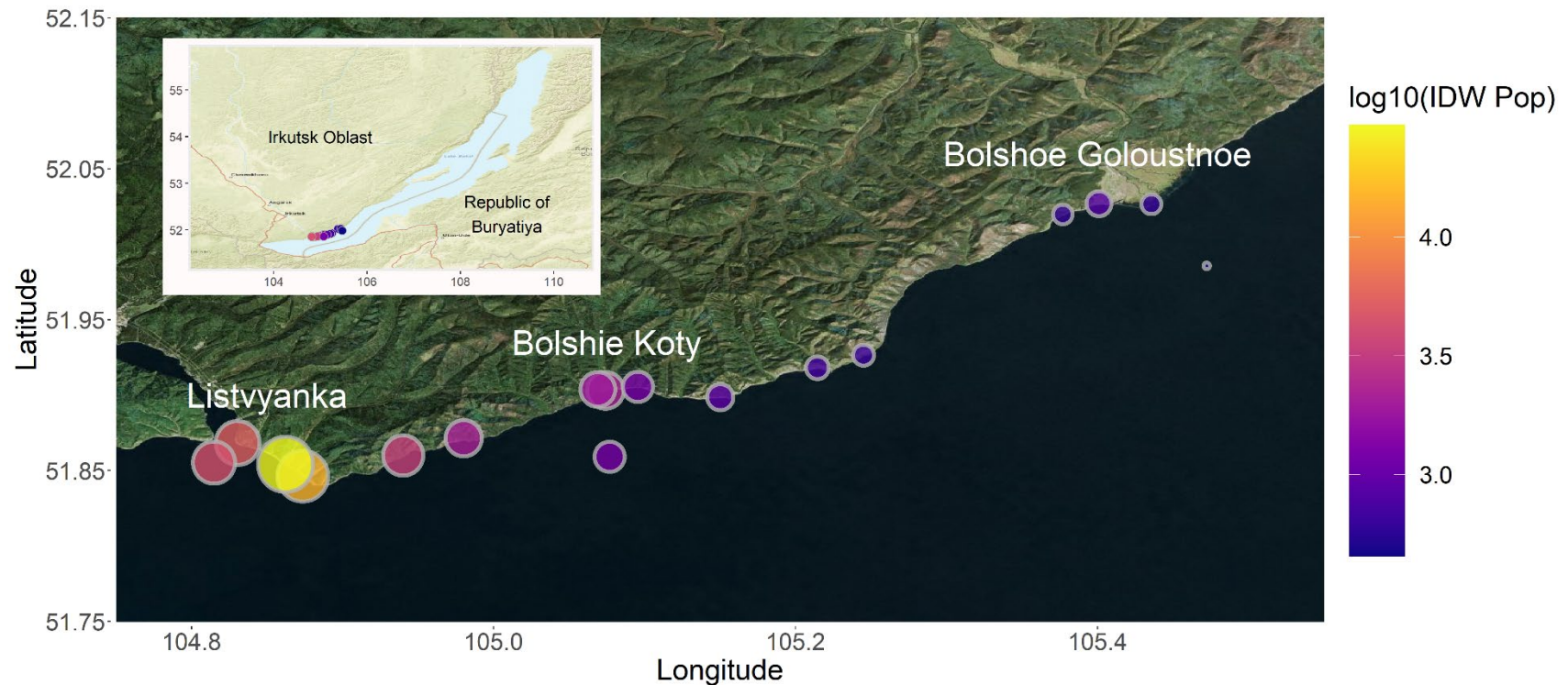
1128 The authors declare no conflicts of interest.

Table 1: Location, depth, temperature and population information for each of the 17 sampling stations. “OS” refers to pelagic locations (i.e., “Offshore”), whereas other site abbreviations refer to littoral sampling locations.

Site	Latitude	Longitude	Depth (m)	Distance to shore (m)	Air Temperature (°C)	Surface Temperature (°C)	Adjacent Population
BK-1	51.90316	105.07404	0.7	10	18	14	80
BK-2	51.90365	105.069	0.9	17.5	19	13	80
BK-3	51.90536	105.0957	0.8	10	18	14	80
BGO-1	52.02693	105.40102	0.9	18	20	13	0
BGO-2	52.0197	105.37707	1.1	14	19	14	600
BGO-3	52.02649	105.43577	0.7	21	18	16	600
OS-1	51.98559	105.47237	900	NA	15	NA	NA
KD-1	51.92646	105.24504	0.8	20.75	23	NA	0
KD-2	51.91807	105.21456	0.9	14.5	23	16	0
MS-1	51.89863	105.15017	0.6	10.5	21	17	0
SM-1	51.87152	104.98006	0.9	11.5	21	15	0
LI-1	51.86825	104.83042	0.6	8.9	19	14	2000

LI-2	51.84626	104.87356	0.8	9.4	21	15	2000
LI-3	51.85407	104.86216	0.7	9.25	19.5	15	2000
EM-1	51.86005	104.93999	0.7	15.5	24.5	14	0
OS-2	51.8553	104.8148	1300	NA	21	NA	NA
OS-3	51.859108	105.0769	1400	5000	NA	14.5	NA

1130



1131

1132 Figure 1: Map of all sampling locations with sites sized and colored by log-transformed IDW population. IDW population was log-
1133 transformed so as to make IDW populations across three orders of magnitude more comparable. The entire transect included three
1134 developed sites (i.e., Listvyanka, Bolshie Koty, Bolshoe Goloustnoe). Three offshore samples were also collected to compare pelagic
1135 sewage signals to those in the littoral. Sampling locations west of Listvyanka are located farther from Listvyanka's centroid, and
1136 therefore have lower IDW population values than sites located closer to the centroid. This map was created using the R statistical

1137 environment (R Core Team 2019) and the tidyverse (Wickham et al. 2019), OpenStreetMap (Fellows and Stotz 2019), ggpubr

1138 (Kassambara 2019), cowplot (Wilke 2019), and ggrepel (Slowikowski 2019) packages.

1139

1140



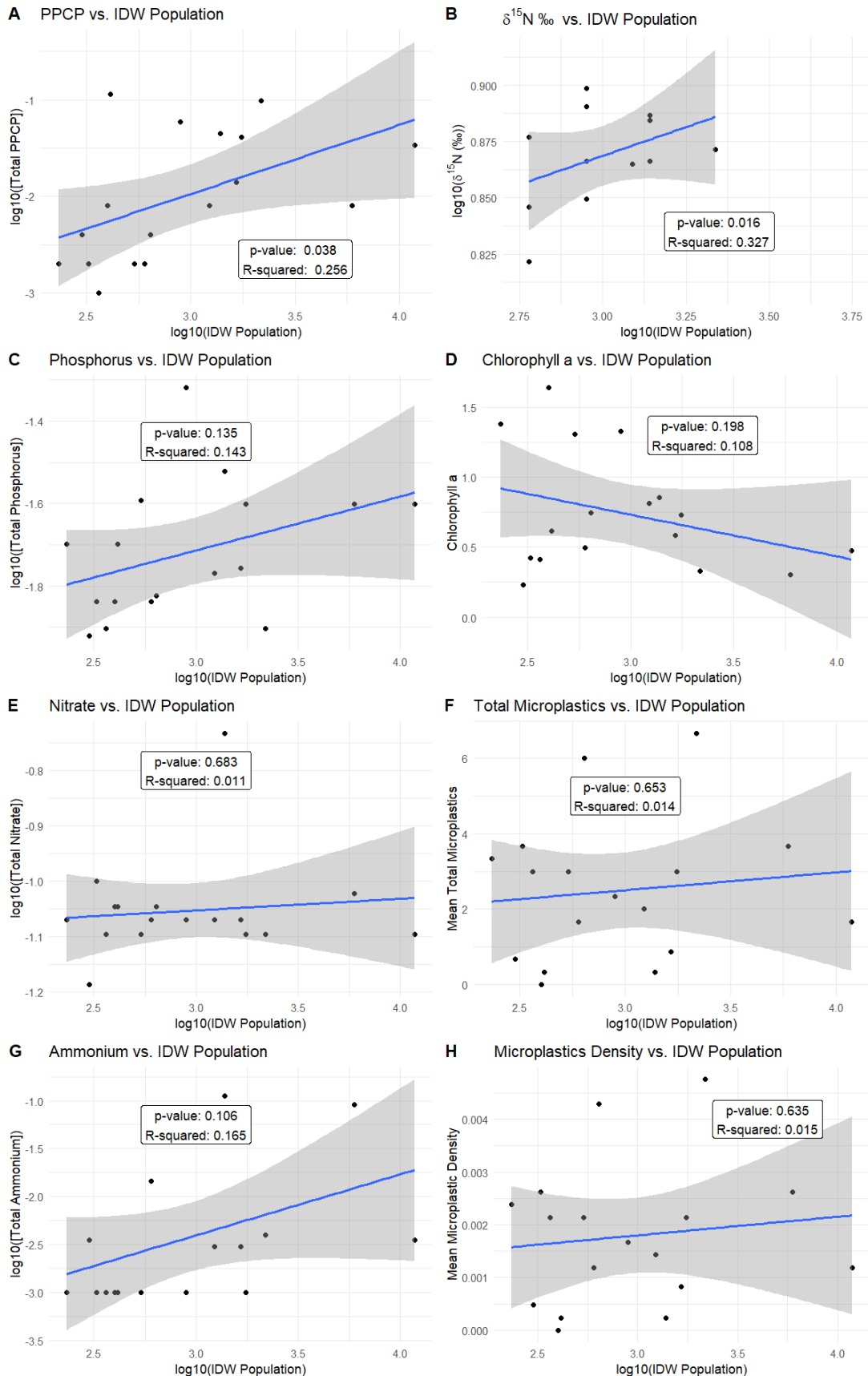
1141

Listvyanka (1,963 pop.)

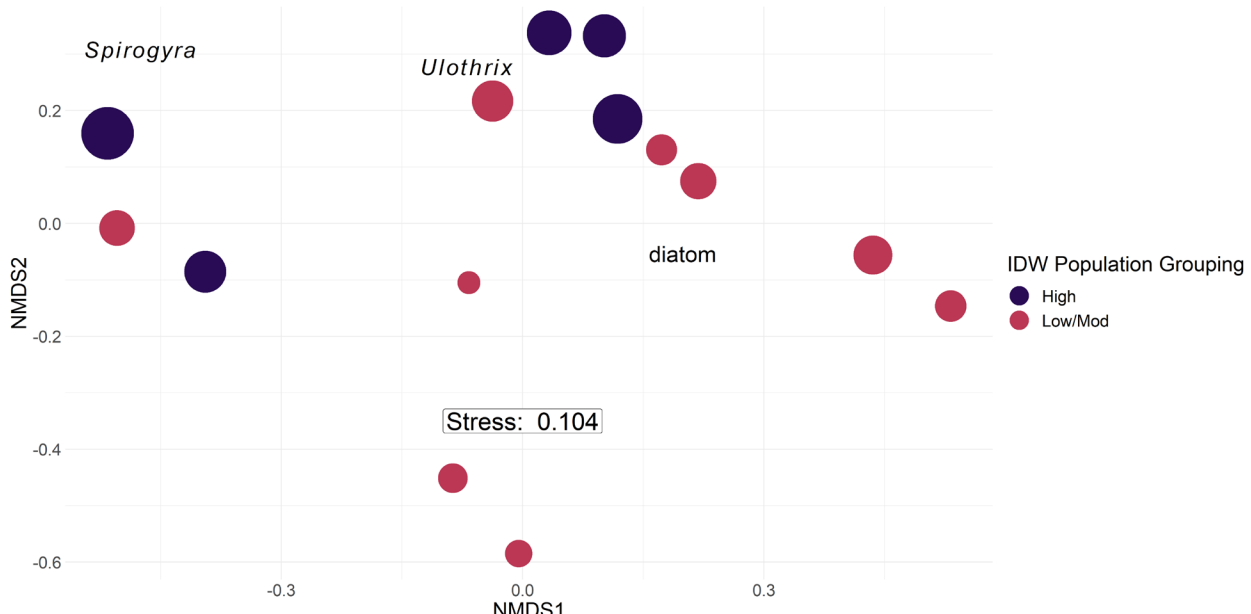
1142 Figure 2: Photographs and Google Earth imagery of each developed area. Photographs were
1143 taken by Kara H. Woo and Michael F. Meyer.

Table 2: Average sewage indicator concentrations and densities per sampling location. Caffeine, acetaminophen/paracetamol, paraxanthine, and cotinine detection limits are estimated to be 0.001 µg/L based on a 500 mL sample volume.

Site	NH ₄ ⁺ (mg/L)	NO ₃ ⁻ (mg/L)	Total Phosphorus (mg/L)	Caffeine (µg/L)	Acetaminophen (µg/L)	Paraxanthine (µg/L)	Cotinine (µg/L)	Fragment density (MPs/L)	Fiber density (MPs/L)	Bead density (MPs/L)	IDW population	Categorical IDW population
BK-1	0.003	0.085	0.054	0.011	0.001	0.002	0	0	0.000833	0	2304.039	High
BK-2	0.003	0.085	0.052	0.007	0.001	0	0	0.000952	0.000476	0	1891.558	Mod/Low
BK-3	0.068	0.09	0.045	0.003	0.001	0	0	0.003095	0.00119	0	1231.234	Mod/Low
BGO-1	0.0145	0.085	0.044	0	0.002	0	0	0.00119	0	0	838.5385	Mod/Low
BGO-2	0.001	0.08	0.0385	0	0.001	0	0	0.000238	0.001905	0	611.91	Mod/Low
BGO-3	0.001	0.09	0.044	0.005	0.003	0	0	0	0	0	624.455	Mod/Low
OS-1	0.001	0.085	0.061	0	0.001	0	0.001	0.002381	0	0	455.7733	Mod/Low
KD-1	0.0035	0.065	0.0375	0.003	0.001	0	0	0	0.000476	0	662.4151	Mod/Low
KD-2	0.001	0.1	0.0445	0.001	0.001	0	0	0.000714	0.001905	0	720.5484	Mod/Low
MS-1	0.001	0.09	0.061	0.064	0.035	0.015	0	0	0.000238	0	903.6733	Mod/Low
SM-1	0.001	0.085	0.1475	0.042	0.012	0.005	0	0	0.001667	0	2146.218	Mod/Low
LI-1	0.004	0.08	0.0385	0.05	0.04	0.006	0.002	0.00381	0.000238	0.000714	5403.209	High
LI-2	0.091	0.095	0.0775	0.001	0.007	0	0	0.001429	0.00119	0	14792.51	High
LI-3	0.0035	0.08	0.077	0.027	0.002	0.002	0.003	0.000476	0	0.000714	29511.73	High
EM-1	0.1125	0.185	0.092	0.029	0.014	0.002	0	0	0.000238	0	3389.949	High
OS-2	0.001	0.08	0.078	0.033	0.001	0.004	0.003	0.000238	0.001905	0	4340	High
OS-3	0.001	0.08	0.0795	0.001	0.001	0	0	0	0.002143	0	1221.424	Mod/Low



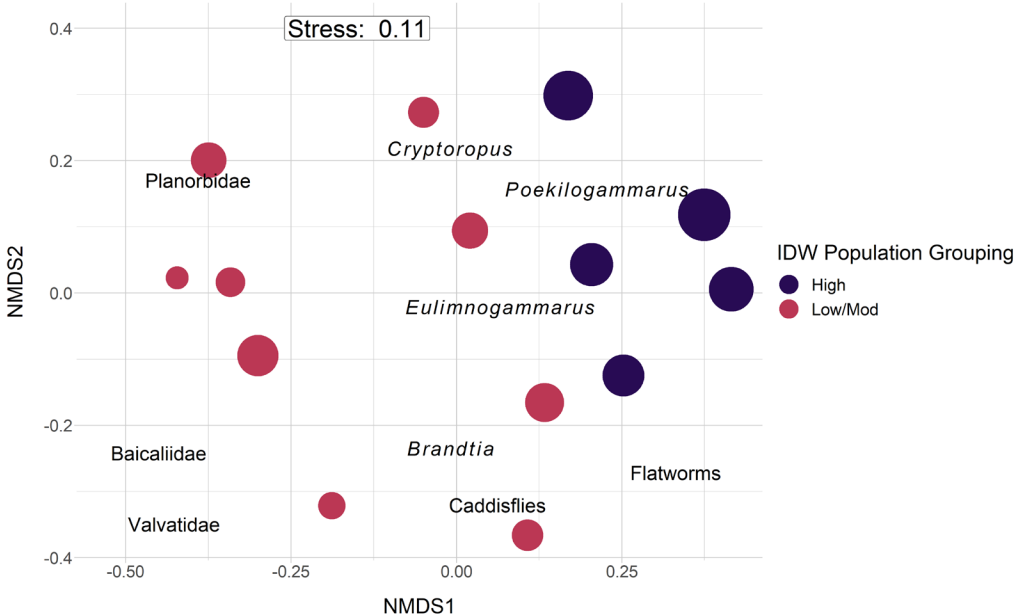
1146 Figure 3: Linear models of total PPCP concentrations (A), macroinvertebrate $\delta^{15}\text{N}$ (B), total
1147 phosphorus (C), chlorophyll a (D), nitrate (E), total microplastics (F), ammonium (G), and
1148 microplastic density (H) regressed against log-transformed inverse distance weighted (IDW)
1149 population. Total PPCP concentrations (A) and macroinvertebrate $\delta^{15}\text{N}$ (B) produced significant
1150 models. Total phosphorus (C), chlorophyll a (D), nitrate (E), total microplastics (F), ammonium
1151 (G), and microplastic density (H) did not produce significant models.



1152

1153 Figure 4: Periphyton abundance NMDS with Bray-Curtis dissimilarity. Points are sized by log10
 1154 IDW population and colored by grouped IDW population values. Taxonomic labels represent
 1155 species scores, which are weighted averages of species contributions from site scores. For
 1156 periphyton, PERMANOVA ($p = 0.001$) and post-hoc SIMPER results suggested sites with a
 1157 higher IDW population value tended to be more associated with filamentous algal groupings and
 1158 separate from sites with moderate and low IDW population values, which were more associated
 1159 with diatom abundance.

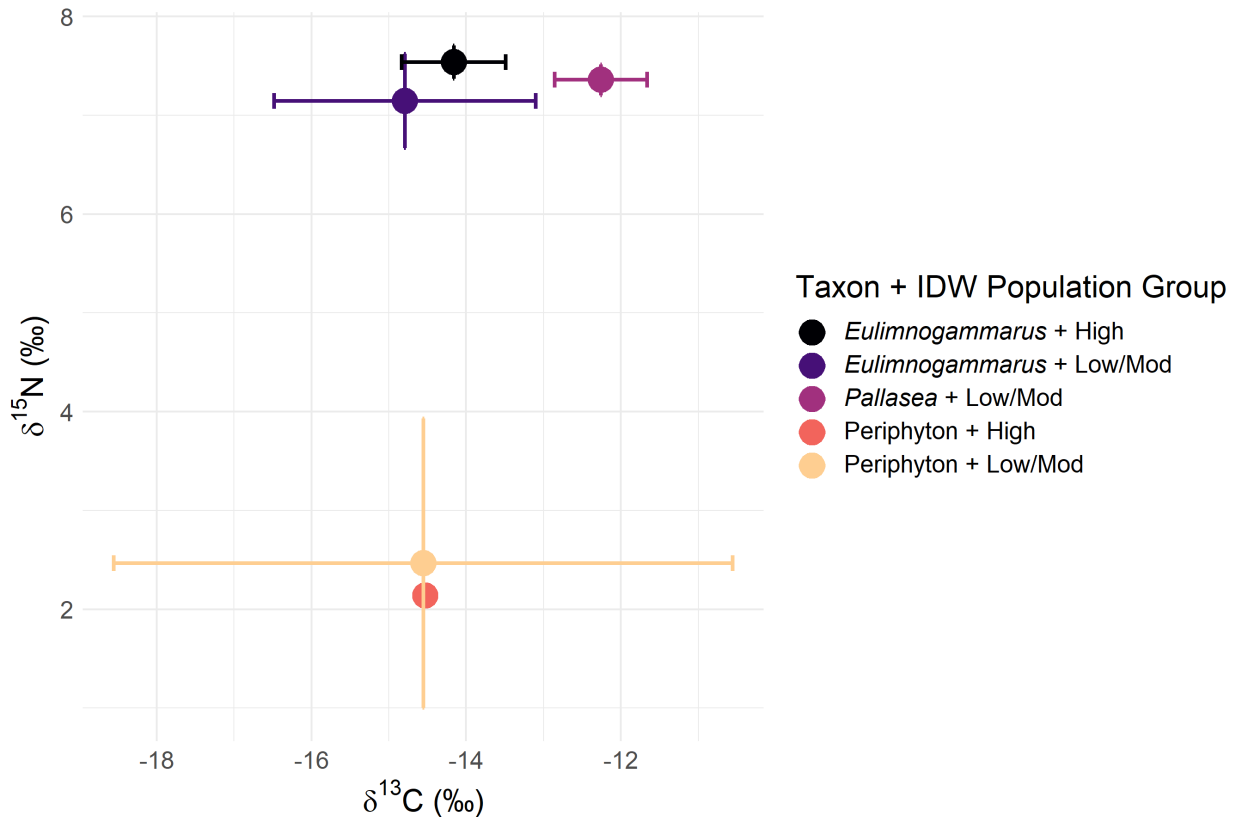
1160



1161

1162 Figure 5: Macroinvertebrate abundance NMDS with Bray-Curtis dissimilarity. Points are sized
 1163 by log10 IDW population and colored by grouped IDW population values. Taxonomic labels
 1164 represent species scores, which are weighted averages of species contributions from site scores.
 1165 For macroinvertebrates, PERMANOVA ($p = 0.02$) and post-hoc SIMPER results suggested sites
 1166 with a higher IDW population values tended to be associated with amphipod taxa (see Table S1),
 1167 whereas sites with lower and moderate IDW population values were more associated with
 1168 increased mollusk abundance (see Table S1).

1169



1170

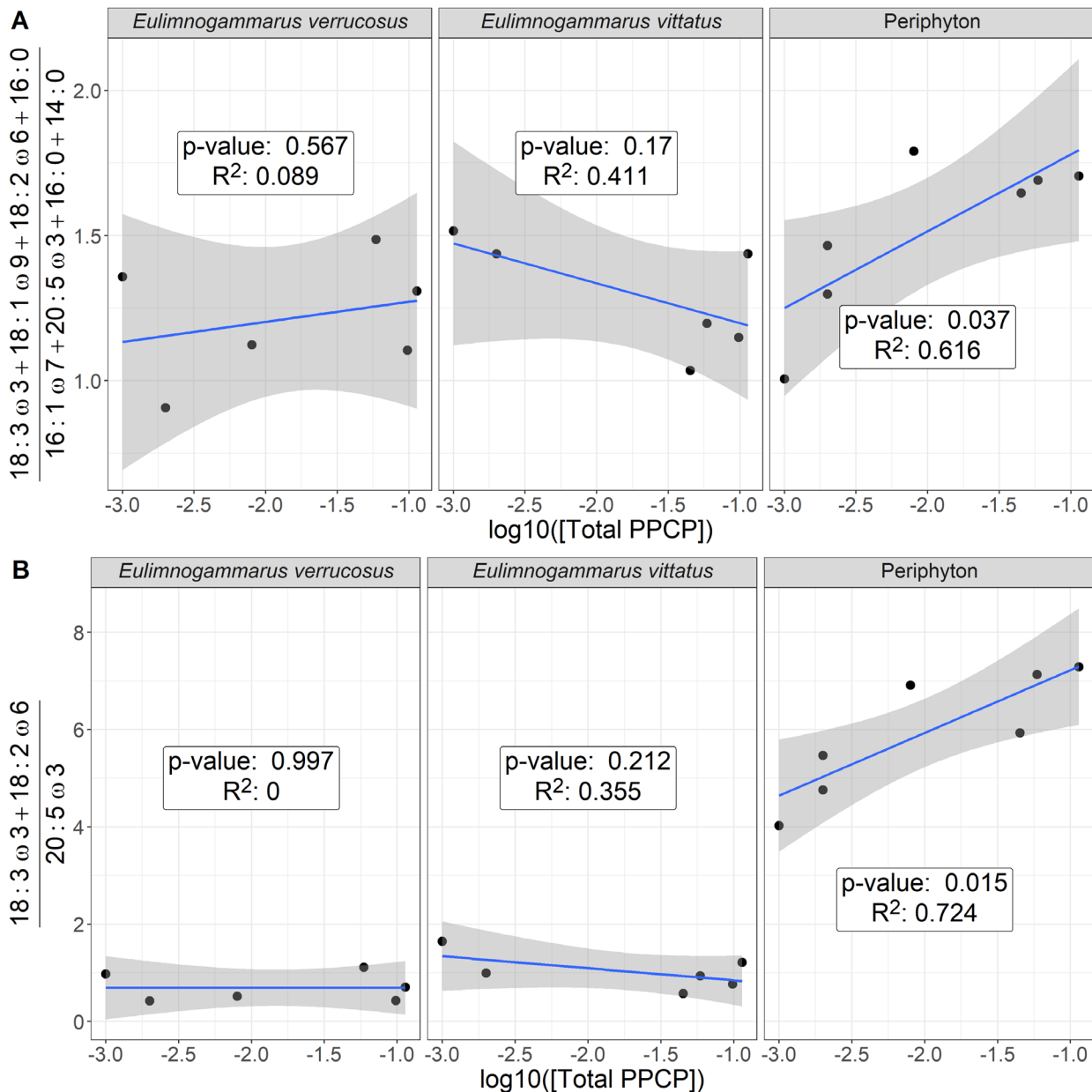
1171

1172 Figure 6: Biplot of mean and standard deviation $\delta^{13}\text{C}$ and $\delta^{15}\text{N}$ stable isotope values for littoral
 1173 amphipods and periphyton, grouped by categorical IDW population (Table 2). In general,
 1174 periphyton did not differ in $\delta^{13}\text{C}$ or $\delta^{15}\text{N}$ signatures with increasing IDW population, whereas
 1175 *Eulimnogammarus* amphipods increased in $\delta^{15}\text{N}$ signatures with increasing IDW population.
 1176 *Pallasea* signatures differed from *Eulimnogammarus* most likely because *Pallasea* tends to
 1177 remain in the nearshore area, whereas *Eulimnogammarus* will regularly migrate to deeper zones
 1178 (Takhteev & Didorenko, 2015).

1179

Table 3: Mean inter-site fatty acid proportion of each taxon and fatty acid grouping (as defined in Table S2).

Taxon	Number of sites	Branched	LCPUFA	MUFA	SAFA	SCPUFA
<i>Draparnaldia</i> spp.	4	0.000	0.012	0.088	0.189	0.710
<i>Eulimnogammarus cyaneus</i>	2	0.002	0.259	0.309	0.248	0.182
<i>Eulimnogammarus verrucosus</i>	6	0.000	0.188	0.385	0.240	0.187
<i>Eulimnogammarus vittatus</i>	6	0.001	0.171	0.371	0.241	0.216
<i>Pallasea cancellus</i>	3	0.001	0.282	0.359	0.187	0.171
Periphyton	7	0.000	0.073	0.092	0.284	0.550
Snail	3	0.002	0.470	0.123	0.194	0.211



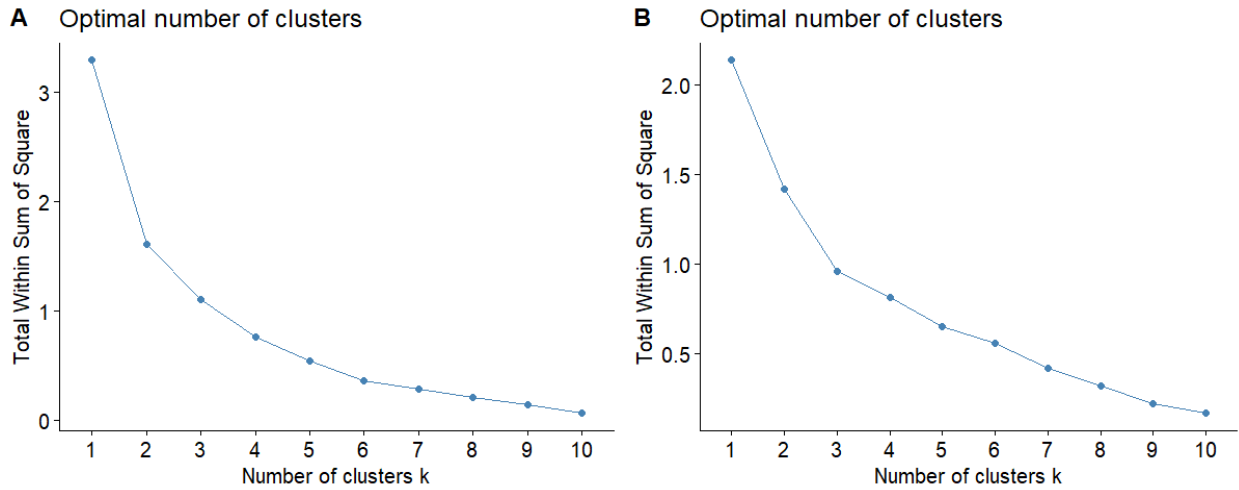
1183 Figure 7: Ratio of filamentous:diatom-associated fatty acids (A) and essential fatty acids (B)
 1184 across our PPCP gradient. Our first analysis (A) focused solely on green filamentous algal fatty
 1185 acids (i.e., 18:3ω3, 18:1ω9, 18:2ω6, and 16:0 relative to diatom fatty acids (i.e., 20:5ω3, 16:1ω7,
 1186 16:0, 14:0) in relation to increasing PPCP concentrations. This first analysis suggested
 1187 periphyton reflected an increasing green, filamentous signature relative to diatoms, which

1188 corroborates analyses showing community compositional shifts (Figure 4). While periphyton
1189 fatty acids changed significantly across our sewage gradient, macroinvertebrate signatures
1190 remained consistent. Our second analysis (B) focused solely on the essential fatty acids, which
1191 further highlights the trends observed in periphyton and macroinvertebrate grazers.

Table S1: Macroinvertebrate taxonomic groupings for abundance estimates. Amphipod taxa were defined as in Takhteev & Didorenko, 2015; mollusk taxa were defined as in Sitnikova, 2012.

Amphipoda	Mollusca	Other
<i>Brandtia latissima intermida</i> (Dorogostaiskii 1930)	Acroloxidae	Asellidae
<i>Brandtia latissima lata</i> (Dybowsky 1874)	Baicaliidae	Caddisflies
<i>Brandtia latissima latior</i> (Dybowsky 1874)	Benedictidate	Hirudinea
<i>Brandtia latissima latissima</i> (Gerstfeldt 1858)	Maackia	Planaria
<i>Brandtia parasitica parasitica</i> (Dybowsky 1874)	Planorbidae	
<i>Cryptoropuss inflatus</i> (Dybowsky 1874)	Valvatidae	
<i>Cryptoropuss pachytus</i> (Dybowsky 1874)		
<i>Cryptoropuss rugosus</i> (Dybowsky 1874)		
<i>Eulimnogammarus capreolus</i> (Dybowsky 1874)		
<i>Eulimnogammarus cruentus</i> (Dorogostaiskii 1930)		
<i>Eulimnogammarus cyaneus</i> (Dybowsky 1874)		
<i>Eulimnogammarus grandimanus</i> (Bazikalova 1945)		
<i>Eulimnogammarus maacki</i> (Gerstfeldt 1858)		
<i>Eulimnogammarus maritui</i> (Bazikalova 1945)		
<i>Eulimnogammarus verucossus</i> (Gerstfeldt 1858)		
<i>Eulimnogammarus viridis viridis</i> (Dybowsky 1874)		
<i>Eulimnogammarus vittatus</i> (Dybowsky 1874)		
<i>Pallasea brandtia brandtia</i> (Dybowsky 1874)		
<i>Pallasea brandtii tenera</i> (Sovinskii 1930)		

<i>Pallasea cancelloides</i> (Gerstfeldt 1858)		
<i>Pallasea cancellus</i> (Pallas 1776)		
<i>Pallasea viridis</i> (Garjajev 1901)		
<i>Poekilogammarus crassimus</i> (Sovinskii 1915)		
<i>Poekilogammarus ephippiatus</i> (Dybowsky 1874)		
<i>Poekilogammarus megonychus perpolitus</i> (Takhteev 2002)		
<i>Poekilogammarus pictus</i> (Dybowsky 1874)		

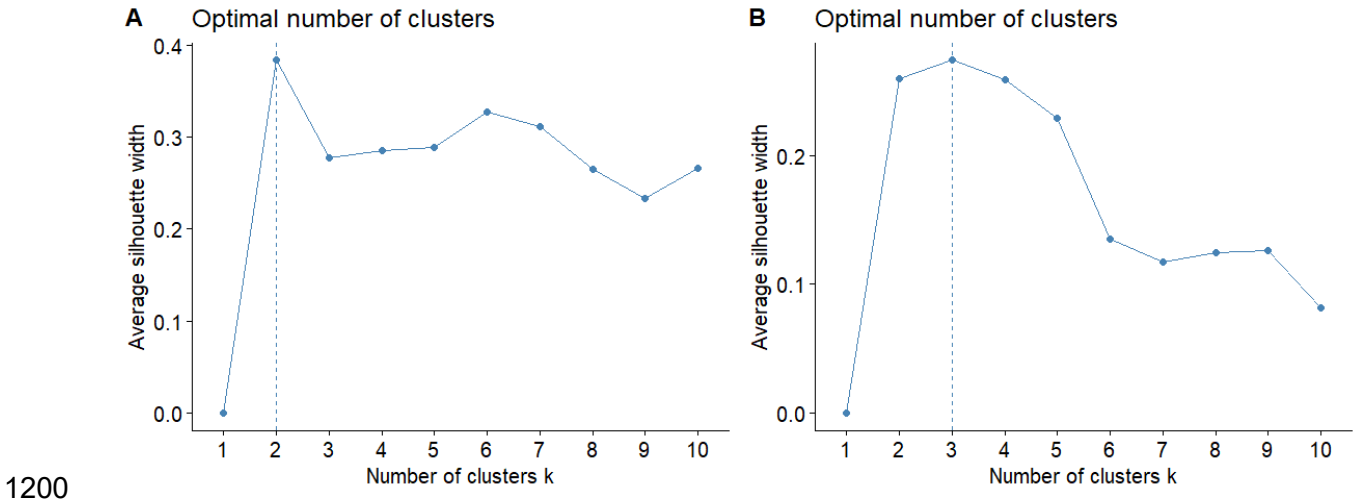


1193

1194

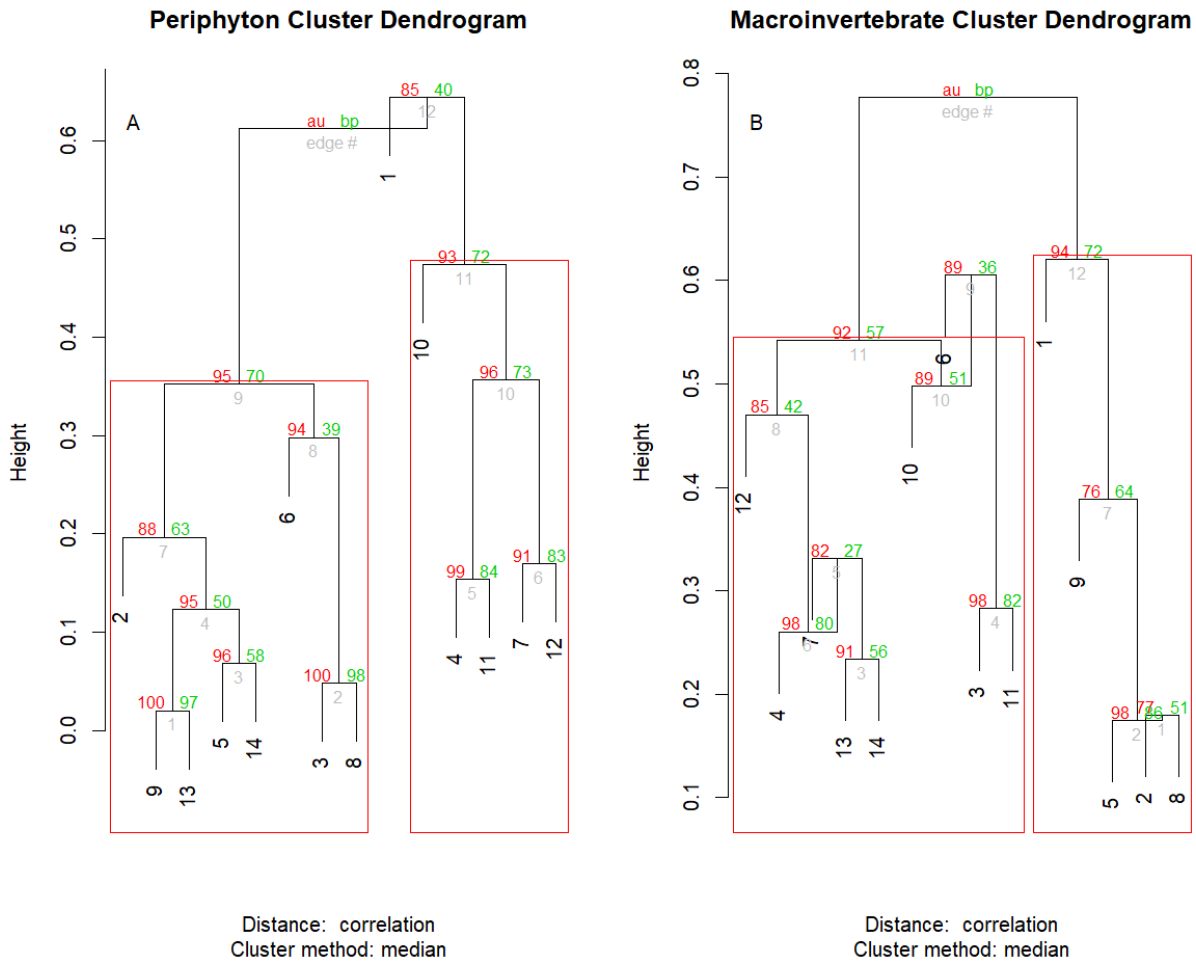
1195 Figure S1: With-group-sum-of-squares (wss) for increasing number of k-mediod clusters for
 1196 periphyton (A) and invertebrate (B) community data. In the case of periphyton data, wss
 1197 decreases most markedly with three clusters, whereas invertebrate community abundance is best
 1198 described by potential two or three clusters.

1199



1200
1201 Figure S2: Average silhouette width for increasing number of k -mediod clusters for periphyton
1202 (A) and invertebrate (B) community data. In the case of periphyton data, average silhouette
1203 width decreases most markedly with three clusters, whereas invertebrate community abundance
1204 is best described by two or three clusters as the average silhouette width for both two and three
1205 clusters was highest before beginning to decrease.

1206

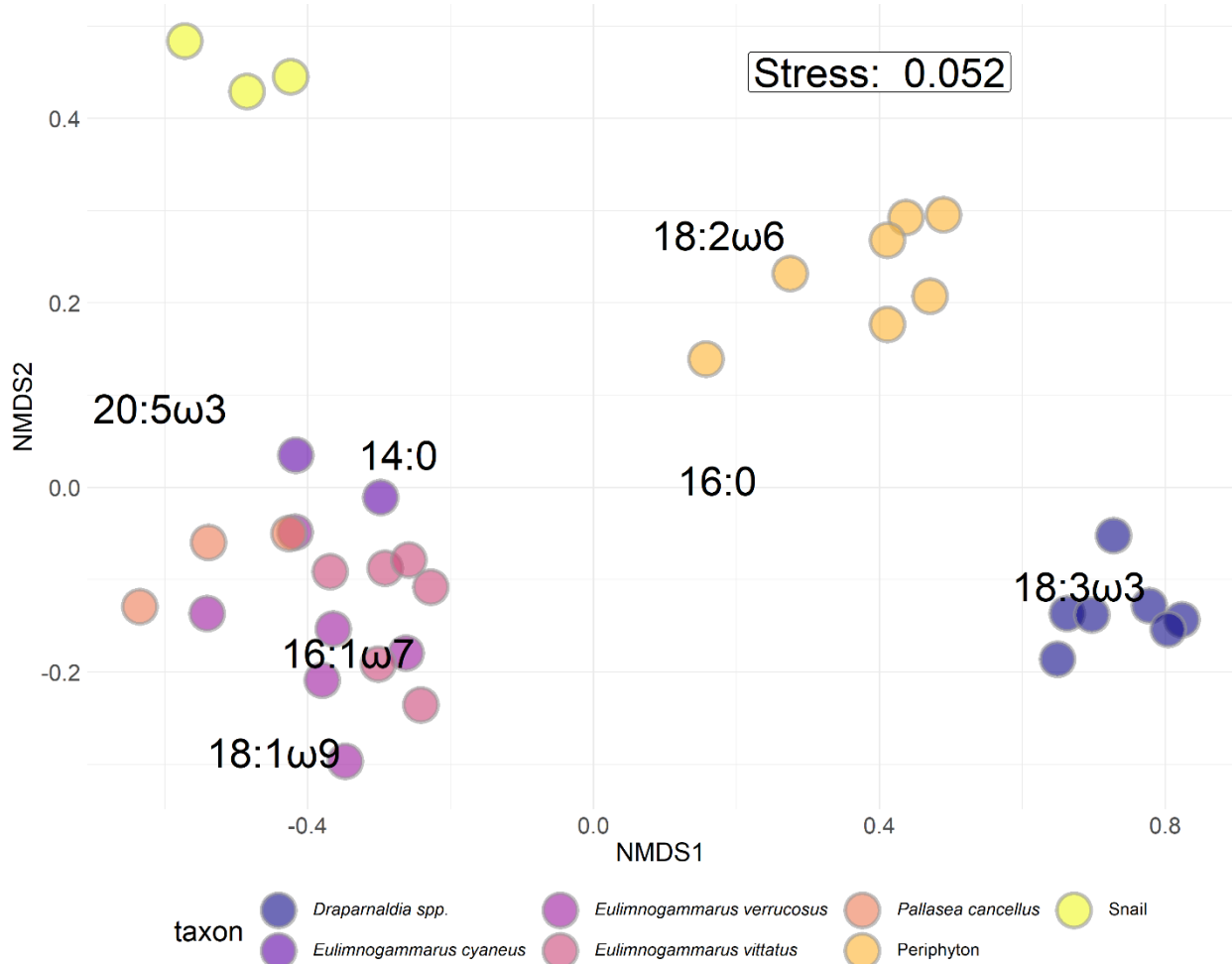


1207

1208 Figure S3: Weighted Pair-Group Centroid Clustering (WPGMC) for periphyton (A) and
 1209 macroinvertebrate (B) community compositions. Approximately unbiased (au) p-values are
 1210 computed by multiscale bootstrap resampling, and displayed in red on the left side of each node.
 1211 Bootstrapped probabilities (bp) are displayed in green on the right side of each node. Unlike k-
 1212 medioids, WPGMC uses a hierarchical approach to assign clusters, which are bootstrapped in
 1213 order to generate a probability of group membership. This technique suggested that both
 1214 periphyton and macroinvertebrates could be grouped in two clusters. Grouping
 1215 macroinvertebrates into three clusters was possible; however, three clusters resulted in 8 of the

1216 14 sampling locations being assigned to a group. In contrast, two groups enabled 13 of the 14
1217 sampling locations to be assigned to a cluster.

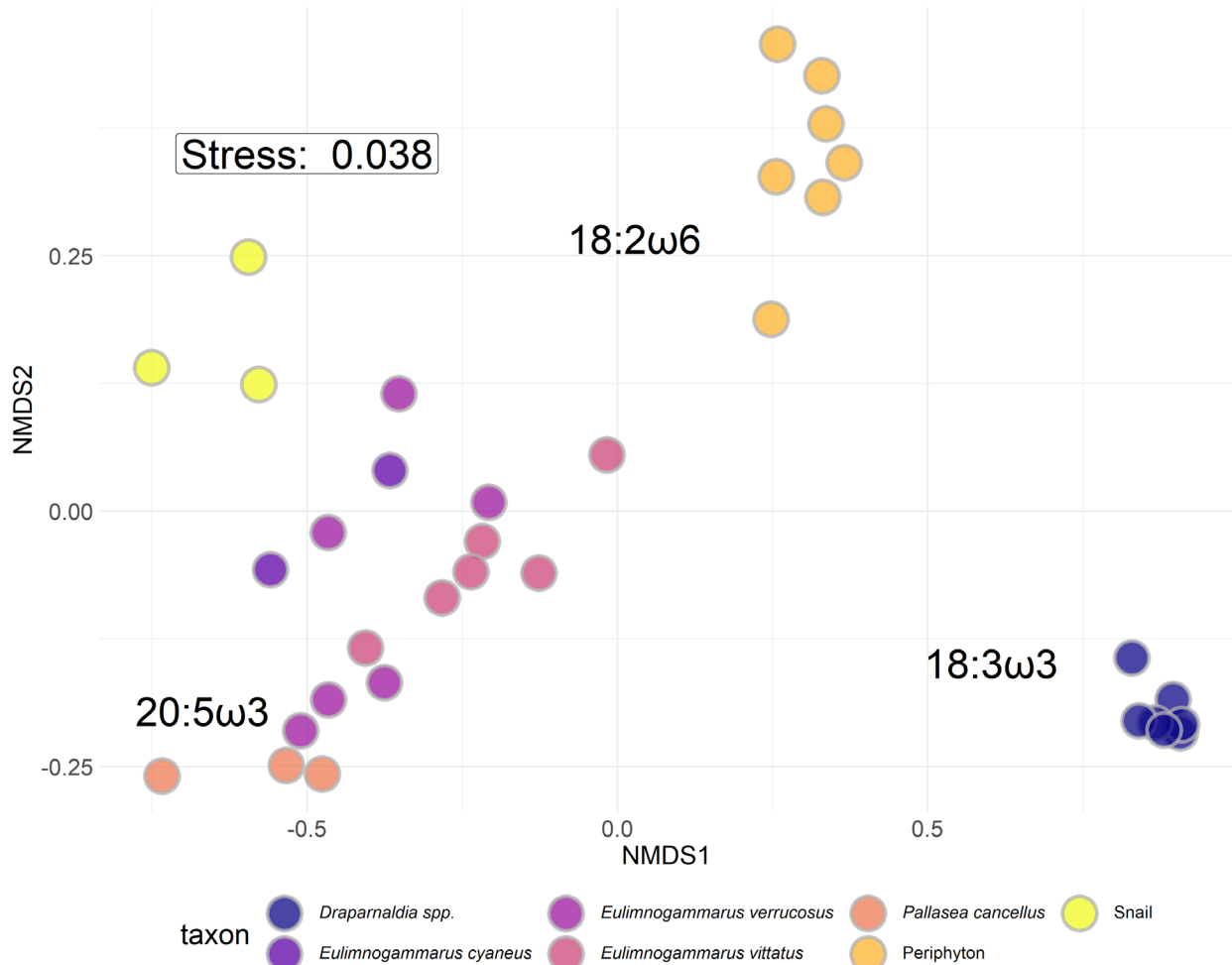
NMDS with Entire FA Spectrum



1218

1219 Figure S2: NMDS with Bray-Curtis dissimilarity of proportional fatty acid compositions for each
 1220 macroinvertebrate and primary producer collected. *Eulimnogammarus* and *Pallasea* are endemic
 1221 amphipod genera. *Draparnaldia* spp. are endemic filamentous algae that are large and form very
 1222 dense mats easily collected where it occurs. *Draparnaldia* spp. occurred in large, visible
 1223 colonies, allowing us to sample and analyze just the *Draparnaldia* spp. fatty acids. Because
 1224 *Draparnaldia* spp. fatty acids were dominated by 18:3 ω 3 more so than periphyton, they formed
 1225 their own cluster. Snails were not identified to species prior to fatty acid analysis. Interspecific
 1226 variation in fatty acid composition tended to be larger than intraspecific variation, implying that
 1227 fatty acid signatures were largely species-specific and not environmentally driven.

NMDS with Essential FA Spectrum



1228

1229 Figure S3: NMDS with Bray-Curtis dissimilarity of proportional biologically essential fatty acid
 1230 compositions for each macroinvertebrate and primary producer collected. *Eulimnogammarus* and
 1231 *Pallasea* are endemic amphipod genera. *Draparnaldia* spp. are endemic filamentous algae that
 1232 are large and form very dense mats easily collected where it occurs. *Draparnaldia* spp. occurred
 1233 in large, visible colonies, allowing us to sample and analyze just the *Draparnaldia* spp. fatty
 1234 acids. Because *Draparnaldia* spp. fatty acids were dominated by 18:3 ω 3 more so than
 1235 periphyton, they formed their own cluster. Snails were not identified to species prior to fatty acid
 1236 analysis. Interspecific variation in fatty acid composition tended to be larger than intraspecific

1237 variation, implying that fatty acid signatures were largely species-specific and not
1238 environmentally driven.

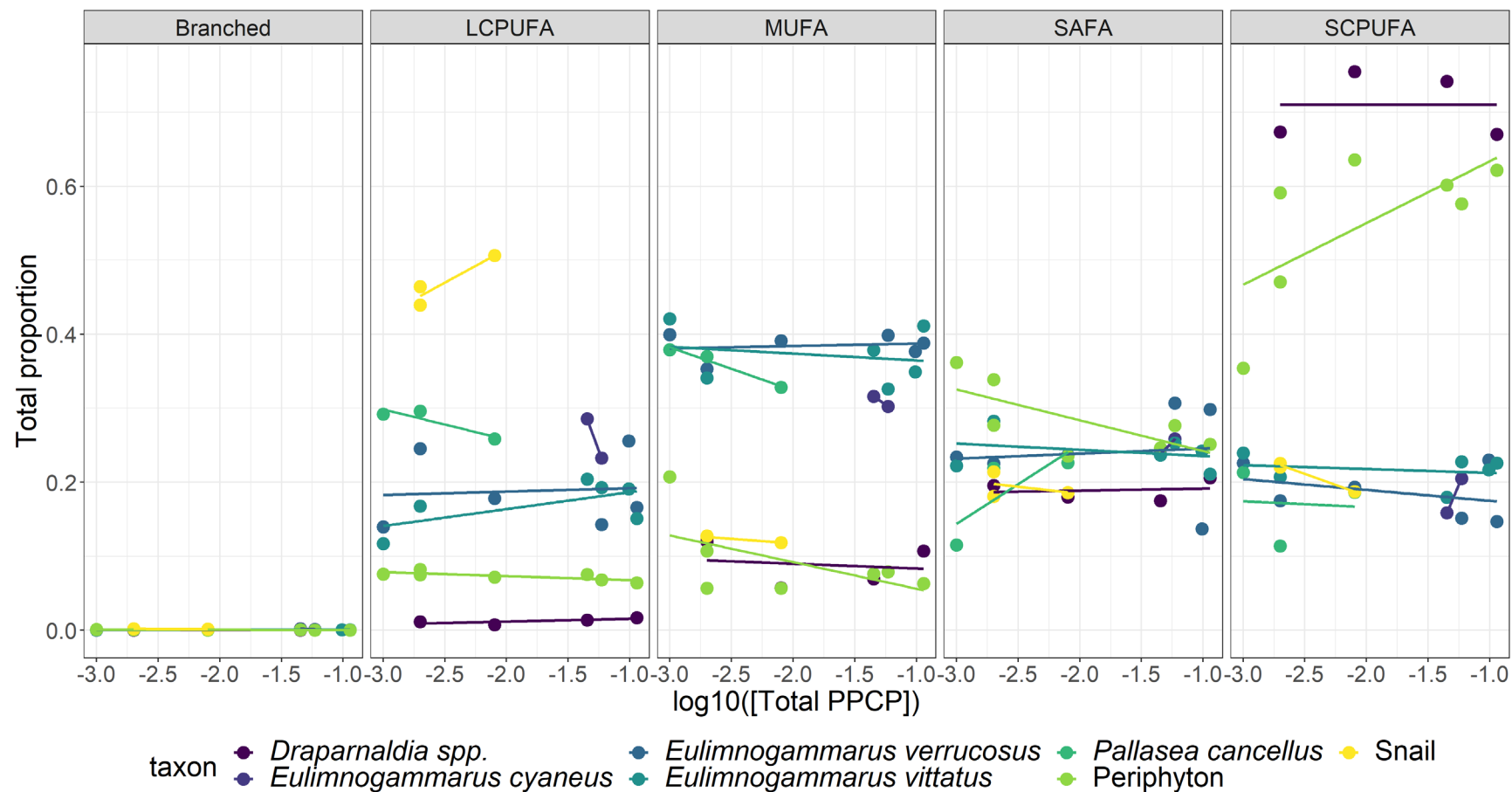
1239

Table S2: Fatty acid groupings used in this analysis

Fatty Acid Group	Fatty acids considered
Branched	a-15:0, i-15:0, a-17:0, i-17:0
SAFA	12:0, 14:0, 15:0, 16:0, 17:0, 18:0, 20:0, 22:0, 24:0
MUFA	14:1 ω 5, 15:1 ω 7, 17:1n7, 16:1 ω 5, 16:1 ω 6, 16:1 ω 7, 16:1 ω 8, 16:1 ω 9, 18:1 ω 7, 18:1 ω 9, 20:1 ω 7, 20:1 ω 9, 22:1 ω 7, 22:1 ω 9
SCPUFA	16:2 ω 4, 16:2 ω 6, 16:2 ω 7, 16:3 ω 3, 16:3 ω 4, 16:3 ω 6, 16:4 ω 1, 16:4 ω 3, 18:2 ω 6, 18:2 ω 6t, 18:3 ω 3, 18:3 ω 6, 18:4 ω 3, 18:4 ω 4, 18:5 ω 3
LCPUFA	20:2 ω 5(11), 20:2 ω 5(13), 20:2 ω 6, 20:3 ω 3, 20:3 ω 6, 20:4 ω 3, 20:4 ω 6, 20:5 ω 3, 22:2 ω 6, 22:3 ω 3, 22:4 ω 3, 22:4 ω 6, 22:5 ω 3, 22:5 ω 6, 22:6 ω 3

1240

1241



1242

1243 Figure S4: Proportions of major fatty acid groups (as defined in Table S2) across the sewage gradient. Primary producers

1244 (*Draparnaldia* spp. and periphyton) were largely characterized by SCPUFAs, amphipods were largely associated with high MUFA

1245 abundance, and snails were generally characterized with high LCPUFA abundance. Across the sewage gradient, periphyton SCPUFA

1246 tended to increase, which lead to more targeted analyses on which specific fatty acids were increasing. In contrast to periphyton, all

1247 other taxa remained consistent with respect to fatty acid proportions across the sewage gradient.

1248

1249

NMDS with Filamentous:Diatom Fatty Acids

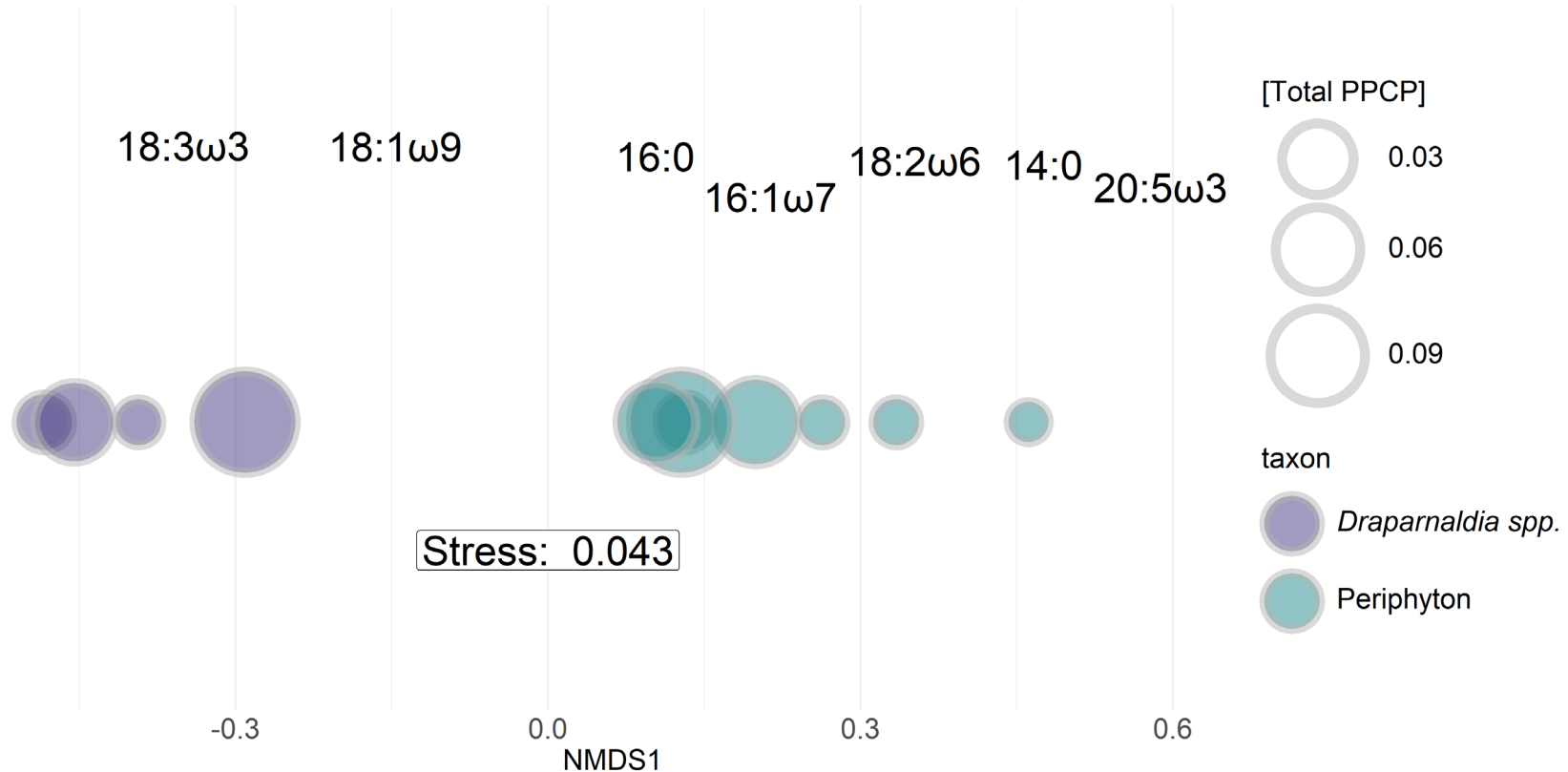
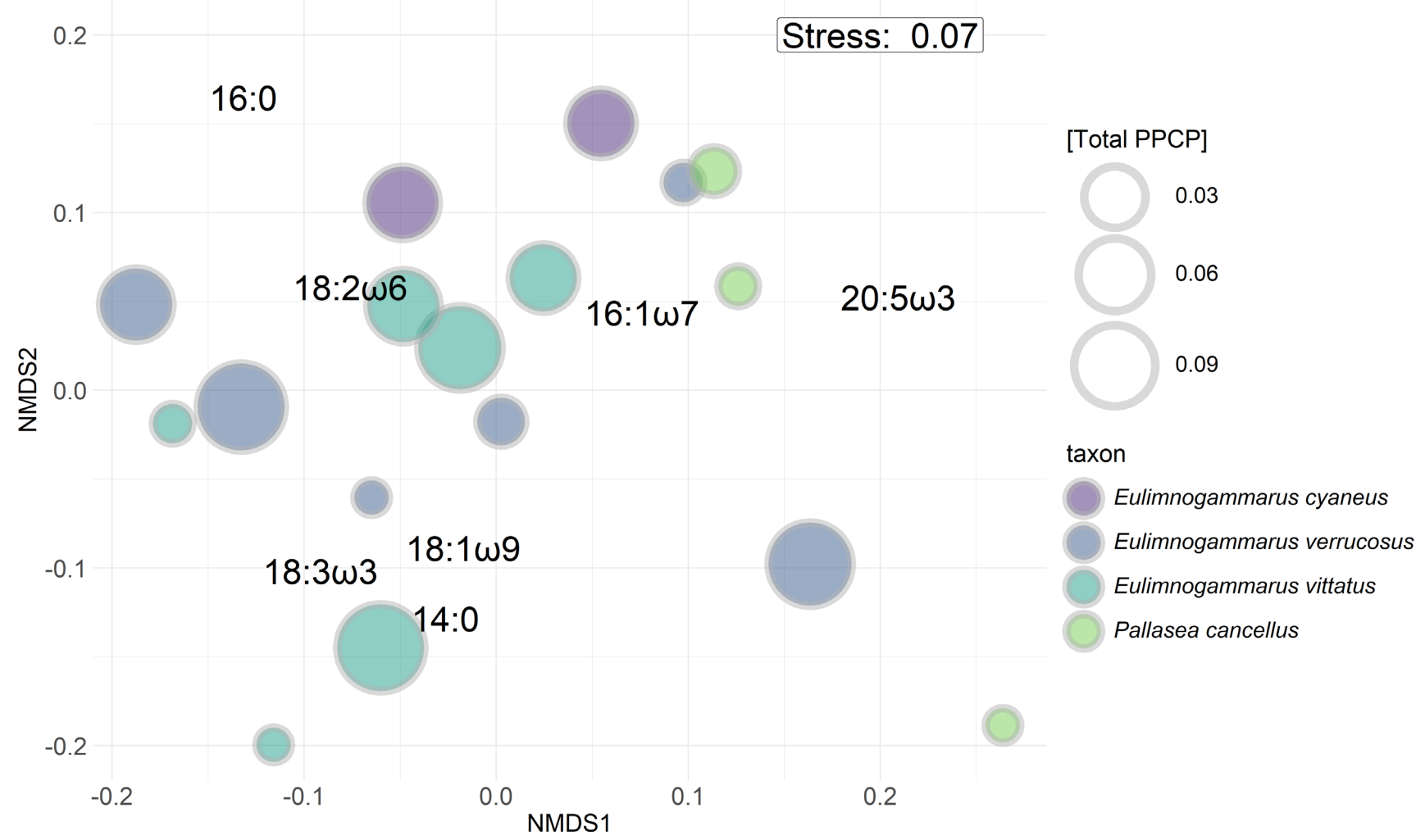


Figure S5: One-dimensional NMDS with Bray-Curtis similarity of seven targeted fatty acids of interest for primary producers. Fatty acid scores are placed above shapes. Shapes are sized by total PPCP concentration. Periphyton (blue-green) tend to increase in size from right-to-left, suggesting that periphyton tend to include more 18:3 ω 3 and 18:1 ω 9 (indicators of green algal taxa) with an increasing sewage signal. In contrast, *Draparnaldia* spp. (purple) fatty acids tend to remain consistent across the sewage gradient.

NMDS with Filamentous:Diatom Fatty Acids



1257 Figure S6: NMDS with Bray-Curtis similarity of seven targeted fatty acids of interest for primary producers. Points are sized by total
1258 PPCP concentration. Visually, there appears to be no distinct separation among or within taxa unlike was observed with periphyton
1259 (Figure S5).

